

國立臺灣大學醫學院微生物學研究所



碩士論文

Graduate Institute of Microbiology

College of Medicine

National Taiwan University

Master Thesis

利用慢性感染之小鼠模式

研究 B 型肝炎病毒專一性免疫功能缺失之機制

Studies of the mechanisms underlying
the immune dysfunction against HBV
in a mouse model of chronic HBV infection

陳致曄

Chih-Yeh Chen

指導教授：陶秘華 博士

Advisor: Mi-Hua Tao, Ph.D.

中華民國一百零二年七月

July, 2013

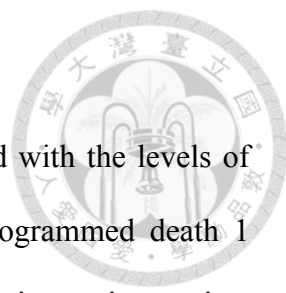
中文摘要



全世界超過三億五千萬的慢性 B 型肝炎病毒感染患者至今仍處於產生肝硬化以及肝細胞癌的高風險之下。清除 B 型肝炎病毒需要有效的 B 型肝炎專一性胞殺型 T 細胞的作用，而專一性胞殺型 T 細胞在急性 B 型肝炎病毒感染的病人中具備有效抗病毒功能，但是在慢性 B 型肝炎病毒感染病人中，這些專一性胞殺型 T 細胞的數目較少，抗病毒功能也較差。臨床報告中，患者體內的 B 型肝炎病毒劑量被指出與專一性胞殺型 T 細胞的數量及功能存在負相關趨勢。而免疫反應缺失與病毒劑量的因果關係尚未完全釐清，主要原因在於臨床研究中無法操控病毒感染的劑量，而 B 型肝炎的自然宿主只有人類、黑猩猩以及樹鼯，缺乏合適的小動物模式用以研究免疫反應缺失的機制。本實驗室近期發展的慢性 B 型肝炎小鼠模式，透過搭載 B 型肝炎病毒基因體的腺相關病毒載體 (AAV/HBV)，使 B 型肝炎病毒能夠長期在小鼠肝細胞中複製並製造病毒抗原。利用此小鼠模式，我們證明 B 型肝炎病毒專一性免疫反應有功能缺失的現象，而較高的病毒劑量確實造成較嚴重的功能性缺失，同時造成胞殺型 T 細胞表現較高量的 Programmed death-1 (PD-1) 等抑制型受器 (inhibitory receptors)。PD-1 配體 (ligand) 基因剔除小鼠 (PD-L1 KO) 於感染 AAV/HBV 之後，專一性胞殺型 T 細胞的功能較野生型小鼠的反應為強，而感染後第二週基因剔除小鼠血清中的 B 型肝炎病毒表面抗原量相較於野生型小鼠顯著下降，顯示 PD-1 訊息傳導對於 B 型肝炎專一性胞殺型 T 細胞免疫功能缺失的重要性。然而當基因剔除小鼠感染高劑量的 AAV/HBV 時，血清中抗原量在第八週回升至與野生型小鼠相同的程度，顯示 PD-1 訊息傳導在高劑量 B 型肝炎病毒感染時僅扮演部分角色。由於此模式中，表現 PD-1 的胞殺型 T 細胞無法以專一性五聚體 (pentamer) 偵測出等量的細胞數，因此以功能性分析與替代性實驗方法證明表現 PD-1 的胞殺型 T 細胞具有 B 型肝炎病毒專一性。本篇研究證明高劑量 B 型肝炎病毒造成較嚴重的專一性胞殺型 T 細胞免疫功能缺失，而 PD-1 訊息傳導在高劑量 B 型肝炎病毒感染的情況中僅佔有部分貢獻。因此本篇研究提供未來慢性 B 型肝炎免疫治療的參考依據，利用阻斷 PD-1 作為慢性 B 型肝炎免疫治療時，患者體內病毒劑量可能對於治療結果產生影響，需將其列入評估。

關鍵字：B 型肝炎病毒、慢性病毒感染、病毒劑量、免疫功能缺失、PD-1

Abstract



The viral burdens in chronic hepatitis B patients are correlated with the levels of functional impairment of specific CD8 T cells, which express programmed death 1 (PD-1), and blocking inhibitory signals PD-1 *ex vivo* augments immunity against hepatitis B virus (HBV). However, due to the limitation of heterogeneity of patients, viral subtypes, and exposure time to viruses, it remains elusive whether the different degrees of T-cell dysfunction are directly induced by the divergence of HBV titers. In addition, the therapeutic effect by blocking PD-1:PD-L1 interaction is yet to be determined under high viral loads. Taking advantage of a mouse model of HBV chronic infection that allows the control of the quantities of monoclonal virus following adeno-associated viral vector delivery of HBV genomic DNA, we demonstrated that the functions of HBV-specific CD8 T cells diminished gradually post infection and T cell dysfunction progressed accompanied with increased viral loads. Consistently, intrahepatic CD8 T cells expressed increasing levels of PD-1 and other inhibitory receptors in a viral load-dependent manner. In PD-L1 KO mice, the functions of specific CD8 T cells were more robust in the early phase of infection, leading to reduced levels of viral antigen. However, activity of anti-HBV T cells sustained only in KO mice with low but not high viral loads, implicating the roles of other immune regulatory factors other than the PD-1:PD-L1 pathway. In addition, the HBV-specificity of PD-1⁺ CD8 T cells were demonstrated by functional assays and alternative approaches. Collectively, our data indicate that the viral load-induced dysfunction of HBV-specific CD8 T cells is partially regulated by PD-1 pathway, and impeding this pathway alone may not be sufficient to control the persistent infection, particularly in high HBV levels.

Keywords: HBV, chronic viral infection, viral loads, immune dysfunction, PD-1

Contents



1. Introduction	1
1.1 Chronic viral infection.....	1
1.1.1 T cell exhaustion.....	2
1.1.2 Inhibitory receptors.....	3
1.1.3 Effects of viral burdens on T cell exhaustion	4
1.2 Hepatitis B virus (HBV)	4
1.2.1 Genomic structure and genotypes.....	4
1.2.2 Viral proteins	5
1.2.3 Replication and life cycle	6
1.2.4 HBV infection.....	7
1.2.5 Immune responses in HBV infection.....	7
1.2.6 Animal models.....	8
1.3 Aim of this study	10
2. Materials and Methods	11
2.1 Animals.....	11
2.2 Adeno-associated viral (AAV) vectors.....	11
2.3 AAV injection.....	12
2.4 Immunization.....	12
2.5 Isolation of splenocytes and intrahepatic lymphocytes	12
2.6 IFN- γ and TNF- α ELISPOT	13
2.7 Serological analysis	13
2.8 Flow cytometric analysis and fluorescence-activating cell sorting (FACS)	14
2.9 <i>In vivo</i> blockade with mAb injection.....	15
2.10 Preparation of bone marrow-derived dendritic cells (BMDCs) and <i>in vitro</i>	

adenovirus infection	15
2.11 <i>In vitro</i> T-cell expansion.....	16
2.12 T cell receptor (TCR) repertoire spectratype analysis.....	16
2.13 Statistics.....	17
3. Results	18
3.1 Negative Effects of Viral Loads on The Function of HBV-Specific CD8 T Cells	18
3.2 Intrahepatic T cells from mice with high viral loads expressed higher levels of inhibitory receptors, especially PD-1	19
3.3 The reduction of viral antigens and ameliorated immune responses in the absence of PD-1:PD-L1 interaction	21
3.4 Loss of viral control and HBV-specific responses of CD8 T cells in high viral load mice even in the absence of PD-1:PD-L1 interaction	21
3.5 Blockade of LAG-3 accelerated the reduction of serum HBsAg in PD-L1 KO mice	23
3.6 Identification of H-2K ^b -restricted epitopes of HBsAg and HBcAg.....	23
3.7 Detection of subdominant clones of HBV-specific CD8 T cells which recognize other HBV epitopes during chronic infection.....	24
3.8 Alternative approaches to demonstrate the HBV-specificity of PD-1 ⁺ CD8 T cells	27
4. Discussion.....	29
4.1 Model advantage.....	29
4.2 Tolerance	30
4.3 Dose effect.....	31
4.4 PD-1 expression and other regulatory factors	32



4.5 Blocking PD-1	33
4.6 HBV-specificity of PD-1 ⁺ CD8 T cells	35
4.7 Conclusion	36
5. References	38
6. Figures	53
7. Tables.....	77



Figures

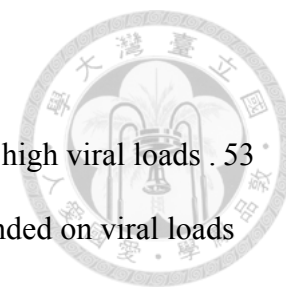
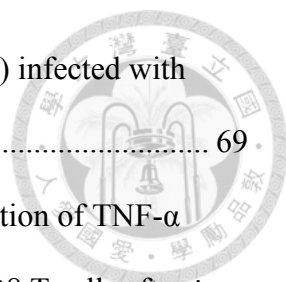


Figure 1. Long-term expression of HBsAg in low, intermediate, and high viral loads .	53
Figure 2. Functional impairment of HBV-specific CD8 T cells depended on viral loads	54
Figure 3. PD-1 expression on intrahepatic CD8 T cells was upregulated in a viral load-dependent manner.....	56
Figure 4. Expression of 2B4 and LAG-3 on intrahepatic CD8 T cells increased with greater extents during infection of higher viral loads.....	58
Figure 5. The levels of PD-1 upregulation on intrahepatic CD4 T cells depended on viral loads	59
Figure 6. HBV-specific immunity in early stage of infection was more potent in the absence of PD-1:PD-L1	60
Figure 7. Reduction of HBsAg in PD-L1 KO mice infected with low, intermediate, and high viral loads of AAV/HBV	61
Figure 8. Higher viral loads elicited more intense functions of HBV-specific CD8 T cells in the early phase of infection in PD-L1 KO mice.....	62
Figure 9. Accelerated functional loss of HBV-specific CD8 T cells in PD-L1 KO mice infected with high viral load of AAV/HBV	63
Figure 10. Blockade of LAG-3 accelerated the reduction of serum HBsAg in PD-L1 KO mice	65
Figure 11. Identification of H-2Kb-restricted dominant epitopes of HBsAg and HBcAg	66
Figure 12. Detection of subdominant clones of HBV-specific CD8 T cells in chronically infected C57BL/6 mice.....	68
Figure 13. PD-1 ⁺ CD8 T cells from AAV/HBV-infected mice were irresponsive to	



stimulation using bone marrow-derived dendritic cells (BMDCs) infected with
adenoviral vectors expressing HBV antigens..... 69

Figure 14. PD-1⁺ intrahepatic CD8 T cells showed more intense function of TNF- α
production against HBV peptides than the PD-1⁻ counterpart CD8 T cells after *in*
vitro expansion 71

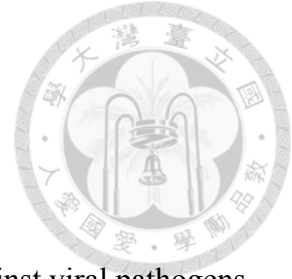
Figure 15. The frequencies of CD11a^{hi} CD8 T cells depended on viral loads of
AAV/HBV 73

Figure 16. Higher degree of oligoclonal T-cell expansion was observed in PD-1⁺
intrahepatic CD8 T cells than that of the PD-1⁻ counterpart CD8 T cells 75

Tables

Table 1. Overlapping peptide library of HBsAg and HBcAg.....	77
Table 2. Primers for TCR β spectratype analysis.....	80





1. Introduction

1.1 Chronic viral infection

In contrast to acute viral infection in which robust immunities against viral pathogens are rapidly elicited and control the viral replication and spread, chronic viral infection is considered a process of equilibrium between virus and host (1). Two fundamental events are required for the establishment of chronic viral infection. First, the invading viruses have to escape from antiviral immunities that eliminate the pathogens. Second, the strength of immune responses must be adjusted to tolerate the presence of foreign antigens without the induction of excessive inflammation, which can cause severe damage to infected tissues. The functionally impaired immunities are generally observed in patients of chronic viral infection, such as human immunodeficiency virus (HIV), hepatitis B virus (HBV) and hepatitis C virus (HCV), in comparison to the antiviral immune responses in patients with acute infection.

During self-limited acute infection, the innate immune responses, including natural killer (NK) cell activity and interferon (IFN) production, are generated at early stage of infection and act as the first line of defense that limits the spread of virus. Thereafter, adaptive immunities, such as B cells, helper T cells (CD4 T cells), and cytotoxic T lymphocytes (CTL, CD8 T cells), are induced and activated through antigen-presenting cells (APCs). The effective adaptive immune responses contribute to the viral clearance by eliminating infected cells and neutralizing free-form viruses. The immunological situation in chronic viral infection is altered that the hosts fail to generate potent immunity against the invading pathogens. The failure of viral clearance is generally attributed to ineffective adaptive immunity, which could result from an active inhibition of immune activation by the virus or a lack of pathogen-associated molecular patterns

(PAMPs) that are required for the induction of immune activation (2).




1.1.1 T cell exhaustion

Researches in chronic viral infection mostly focus on the dysfunction of T cells, which are the main effector in terms of both cellular and humoral immunities against viral infection. T cell dysfunction is generally classified into T cell anergy and T cell exhaustion. Both of types are characterized with the loss of proliferative and cytolytic activity, the incapability of cytokine production, as well as the susceptibility to apoptosis (1, 3). Nevertheless, anergy arises at the time of first encounter of cognate antigens with the stimulation of MHC-peptide complexes (signal 1) in the absence of costimulatory molecules (signal 2), such as B7.1 and B7.2 (3). In contrast, T cell exhaustion is not decided at the first time of antigen exposure but a progressive progress in the context of persistent existence of cognate antigens, which is a common phenotype of chronic viral infection. Exhausted T cells that are virus-specific in chronic carriers of HIV, HBV, and HCV are found to react poorly or even unresponsive to antigen stimulation.

Several regulatory mechanisms that cause T cell exhaustion are found in chronic viral infection: immature APCs that constantly present antigens in the absence of costimulatory signals, inhibitory cytokines such as IL-10 and TGF- β , regulatory cell subsets like regulatory T cells (Tregs), and inhibitory receptors expressed on T cells that generate regulatory signals and counteract T cell activation. Blocking these inhibitory mechanisms could prevent T cell exhaustion and restore the functions of T cells against virus. They are potential targets of immunotherapies for chronic infection in the future (2).

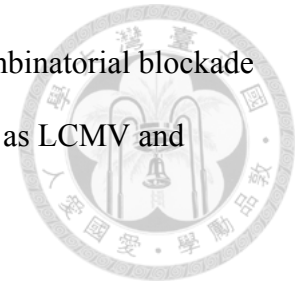
1.1.2 Inhibitory receptors



Recent studies show that in chronic viral infection, inhibitory receptors play critical roles in regulating the immune tolerance, especially in T cell exhaustion (4). Programmed death-1 (PD-1, CD279) is the first inhibitory molecule found essential to T cell exhaustion, as blocking PD-1 signaling restores antiviral functions of virus-specific T cells and help the clearance of persistent virus in chronic lymphocytic choriomeningitis virus (LCMV) infection (5) and in clinical studies of HIV (6). Upon activation, T cells upregulate the expression of PD-1 and thus prevent excessive activation (7). In self-limited infection, the expression of PD-1 is downregulated days after activation. In contrast, the expression is prolonged on T cells in chronic infection, which could be a consequence of constant exposure to antigens (1). When engaging with its ligands, PD-L1 (also as known as B7-H1) and PD-L2 (B7-DC), PD-1 is phosphorylated on its two intracellular, and then binds phosphatases, SHP-1 and SHP-2, that downregulate antigen receptor signaling by dephosphorylation of signaling intermediates (7). PD-L1 has a wider range of expression in parenchymal tissues and hematopoietic cells than that of PD-L2. Blocking PD-1 signaling *in vivo* has not only been shown to have therapeutic effect on animal models of chronic viral infection such as simian immunodeficiency virus (SIV) (8), but also lead to surprising responsive rate in cancer patients of several different types of tumors (9-12).

Other inhibitory receptors, including Lymphocyte activation gene-3 (LAG-3, CD223), Natural killer cell receptor 2B4 (CD244), T cell immunoglobulin (Tim-3) have been identified in LCMV studies and other human chronic viral infection (4, 13-16). They interact with their ligands (LAG-3:MHC II; 2B4:CD48; Tim-3:Galectin-9) and transduce repressive signals that inhibit T cell activation. Individual blockades of these receptors using mAb show positive effects on the rescue of exhausted T cells and the

augmentation of antiviral immunities (4). A synergistic effect of combinatorial blockade of PD-1 and LAG-3 accelerate clearance of chronic pathogens, such as LCMV and plasmodium sp. in animal models (17, 18).



1.1.3 Effects of viral burdens on T cell exhaustion

Studies in LCMV clearly demonstrate that higher viral loads have negative effects on antiviral immune responses. Sustained exposure to high amount of cognate antigens results in the functional impairment of virus-specific CD8 T cells which thus fail to eliminate viral infection (19). In addition, mice with low viral load respond better to therapeutic vaccination (20). High antigen load also can lead to quick loss of memory CD8 T cells (21). In other human disease of chronic viral infection, the negative correlation of viral loads and the antiviral functions of T cells are mostly determined by *in vitro* assays using peripheral blood mononuclear cells (PBMCs) (22, 23), whereas *in vivo* studies are rarely done.

1.2 Hepatitis B virus (HBV)

1.2.1 Genomic structure and genotypes

Hepatitis B virus (HBV) is an enveloped DNA virus with a diameter of 42 nm (Dane particle) and classified taxonomically in hepadnaviridae. The viral genome of HBV is a relaxed circular partially double-stranded DNA with a length of 3.2 kb (24). Negative strand of HBV genomic DNA is in full length and covalently linked with viral polymerase on 5'-end, while positive strand is shorter with a capped oligoribonucleotide on 5'-end. After viral entry, the genomic structure is converted into covalently-closed-circular DNA (cccDNA) in the nucleus of hepatocytes. The viral genome contains 4 open reading frames (ORF) which are highly overlapped: C-ORF,

coding for capsid core protein (HBcAg) and HBV e antigen (HBeAg); P-ORF, coding for HBV polymerase protein; S-ORF, coding for 3 HBV envelope proteins: large surface Ag (pre-S1 or LHBsAg), middle surface Ag (pre-S2 or MHBsAg), and small surface Ag (S, HBsAg, or SHBsAg).

The 4 major RNA transcripts are denominated by their lengths (25). 3.5 kb mRNA includes pregenomic RNA and precore mRNA. The former is responsible for the synthesis of HBcAg and polymerase protein, and serves as the template of for synthesis of DNA negative strand. 2.4 kb mRNA encodes pre-S1 envelope protein and 2.1 kb mRNA is the template for synthesis of pre-S2 envelope protein and HBsAg. 0.7 kb mRNA encodes HBx protein. All the transcripts share the same sequences at 3'-end. At least 8 genotypes, denominated from A to H, have been identified and classified according to an intergroup divergence of more than 8% in the complete nucleotide sequence (26).

1.2.2 Viral proteins

HBcAg is a structural protein with molecular weight of 21 kDa. Dimers of HBcAg comprise the viral nucleocapsids, which encapsidate pregenomic RNA and viral polymerase protein.

HBeAg (precore protein) shares the same ORF with HBcAg with extra 5' sequence, which encodes a signal peptide that direct the newly synthesized precore protein to secretory pathways (27). After cleavage of the N-terminus, the molecular weight of HBeAg decreases from 22 kDa to 17 kDa, smaller than HBcAg. In contrast to HBcAg, which is particulate, HBeAg is non-particulate and secretory. Studies illustrated that HBeAg is dispensable for the replication and infection of HBV (28, 29). However, researches in terms of viral immunology revealed a protective role of HBeAg for HBV

to evade host immunity (30, 31).

HBV polymerase (90 kDa) consists of 3 functional domains: terminal protein (TP) domain, reverse transcriptase (RT) domain, and RNase H domain (RH) (32). TP domain is responsible for protein-priming step of viral replication, while RH domain possesses an enzyme function for digesting the RNA template after reverse transcription by RT domain.

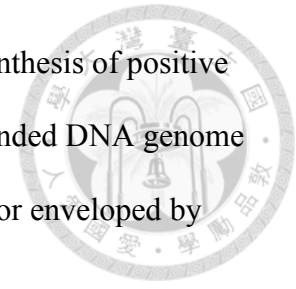
The molecular weights of pre-S1, pre-S2, and S envelope proteins are 39, 33, and 25 kDa, respectively. These proteins share common C-terminal sequences. After synthesized and modified with glycosylation, these proteins are secreted as 22-nm subviral particles, which contain no nucleocapsid of HBV, whereas the 42-nm Dane particles, which are infectious, comprise nucleocapsid. In patients' serum, Dane particles are outnumbered by the non-infectious subviral particles (10^4 to 10^6 folds).

HBx protein has a molecular weight of 17 kDa. HBx protein is inessential for HBV replication but can enhance viral replication (33). Nonetheless, it has been demonstrated that HBx protein can interact with several cellular proteins and regulate their physiological functions, which leads to onsets of hepatocellular carcinoma (HCC) (34).

1.2.3 Replication and life cycle

Hepatocyte is the major tropism of HBV. The putative receptor of HBV has recently been identified and further studies are required to confirm this discovery (35, 36). After the nucleocapsid is transported to the nucleus, the partially double-stranded DNA is converted to cccDNA by cellular DNA polymerase. The episomal cccDNA serves as the template for viral transcripts. After transcription and translation, the pregenomic RNA is bound by viral polymerase and subsequently encapsidated into nucleocapsid, where replication of viral DNA takes place. After reverse transcription by polymerase,

the newly formed negative strand DNA becomes the template for synthesis of positive strand. The mature nucleocapsid containing the partially double-stranded DNA genome is transported back to the nucleus to replenish the pools of cccDNA or enveloped by pre-S1, pre-S2 and HBsAg at a ratio of 1:1:4 followed by secretion.

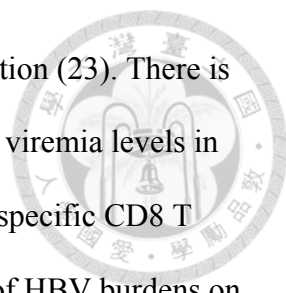


1.2.4 HBV infection

Patients who are serologically positive for HBsAg for more than 6 months are diagnosed as chronic hepatitis B (CHB) infection. More than 350 millions of people worldwide are suffering from chronic hepatitis B infection. HBV infection in adulthood usually becomes asymptomatic and self-limited (90-95%), whereas most neonatal infection via vertical transmission and infection during childhood develop into chronic infection (more than 90%) (37). Additionally, acute HBV infection in persons under immunosuppression conditions is more likely to turn into chronic infection (38).

1.2.5 Immune responses in HBV infection

Persistent infection of hepatitis B virus (HBV) is a common cause of liver cirrhosis and hepatocellular carcinoma worldwide and elucidating the mechanisms of the immunological interaction between HBV and host is the key step toward resolving the diseases (39-41). In acute HBV infection, viral clearance requires specific CD8 T cells which are induced vigorously after exposure to viral antigens and equipped with fully activated antiviral functions, including both cytolytic and non-cytolytic effects that lead to self-limited infection. In contrast, clinical observations of chronic carriers reveal functional defects of HBV-specific CD8 T cells in terms of both quantity and quality. In line with other chronic viral infections, the levels of viremia of chronic HBV patients are inversely correlated to the frequencies of HBV-specific CD8 T cells and their



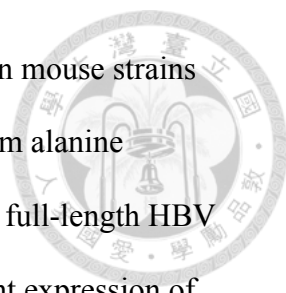
production of cytokines such as IFN- γ which control the viral replication (23). There is a correlation between the expression of PD-1 of these T cells and the viremia levels in patients and blocking PD-1:PD-L1 pathway improve the function of specific CD8 T cells *in vitro* (42). Nonetheless, the investigation of the direct effect of HBV burdens on T cell dysfunction is limited by the diversities of genetic background of patients, viral genotypes, and time of exposure to antigens. It is also difficult to address this issue due to the lack of small animal models of natural chronic HBV infection.

1.2.6 Animal models

Since the natural hosts of HBV are human, chimpanzee, and tupaia, proper animal models with available immunological reagents are absent (43, 44). Several substitutive animal models were developed and used for the research of HBV. Alternative hepadnaviruses that possess infectivity toward hepatocytes of ducks (duck hepatitis B virus, DHBV) and of woodchucks (woodchuck hepatitis virus, WHV) have been used in virological and immunological researches (45, 46). Nevertheless, these viruses differ from HBV and manipulation of experiments of these alternative animals is quite difficult. Immunodeficient mice bearing human hepatocytes as xenografts provide mouse model for virological researches and drug screening. However, the lack of immune system and the laborious experimental procedures render this model limited (47).

HBV-transgenic mice, with HBV genome integrated chromosomally as, were firstly introduced as a mouse model of chronic carrier for the studies of anti-HBV immunity in chronic infection (48, 49). It has a limitation that HBV-specific CD8 T cells are absent in these mice due to central tolerance. As a result, HBV-specific CD8 T cells have to be generated by other donors and adoptively transferred into the transgenic recipients.

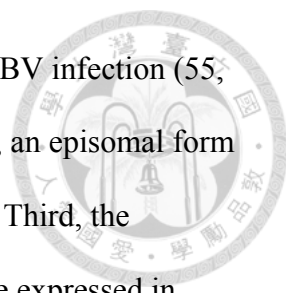
Hydrodynamic injection of plasmids containing terminally redundant HBV genome lead



to chronic infection in part of injected mice (30 to 40%) depending on mouse strains (50). Liver damages are observed in injected mice with elevated serum alanine aminotransferase (ALT). Infection of adenoviral vectors carrying the full-length HBV genome can bypass the viral entry step but can only establish transient expression of HBV. A recent report showed that low dose of adenoviral vectors can achieve long-term HBV replication and protein expression in mouse hepatocytes (51). However, it is difficult to manipulate viral loads in these models due to a relatively narrower window to establish persistent infection.

Using adeno-associated viral (AAV) vectors containing two split genomes of HBV (AAV2/8-5'-HBV-SD and AAV2/8-3'-HBV-SA), we establish persistent viral replication and expression after recombination of two HBV half genomes in the hepatocytes of immunocompetent mice (52). The persistent rate is 100% and independent on mouse strains, as the presence of HBV virions and proteins are detected in the sera and the livers of 4 different strains. The profiles of antibody responses are similar to those observed in chronic carriers, while HBs- but not HBc-specific IFN- γ production of CD8 T cells are detected both in the liver and, to a less extent, the spleen. The frequencies of HBs-reacting CD8 T cells peak at 2 weeks post-infection (p.i.) decrease gradually during persistent infection. The cellular immunity against HBV peaks at week 2 p.i. but diminishes during the persistent expression of virus, indicating a tolerant phenotype to HBV in the immunocompetent hosts. Mice infected with AAV/HBV show hyporesponsiveness to HBV vaccination, but the immunity against ovalbumin (OVA) induced by immunization is comparable to uninfected mice, suggesting the immune tolerance is HBV specific.

There are several advantages of this AAV-mediated mouse model of chronic HBV infection. First, transduction of AAV/HBV shows poor induction of innate immune



responses in immunocompetent hosts (53, 54), which recapitulates HBV infection (55, 56). Second, the AAV DNA genomes are converted into concatamer, an episomal form of extrachromosomal DNA (57), which resembles cccDNA of HBV. Third, the recombinant AAV vectors is defective and no viral genes of AAV are expressed in transduced cells (58). Most importantly, viral loads of HBV in infected hosts can be controlled by adjusting AAV/HBV titers used for infection.

1.3 Aim of this study

In this report, using AAV/HBV-mediated mouse model of chronic HBV infection, we were able to manipulate infectious doses and persistent viral loads in immunocompetent hosts while the infection duration and the homogeneity of host and virus are controlled. We demonstrated that mice expressed and maintained high HBV proteins exhibited a great level of dysfunction of HBV-specific CD8 T cells, concomitant with up-regulation of PD-1 expression. Deprivation of PD-1:PD-L1 signaling partially restored the functions of HBV-specific CD8 T, however, was not sufficient to achieve long-term suppression of HBV in hosts with high viral proteins. Our results suggest that blocking PD-1 signaling alone may not be sufficient to control HBV in chronic carriers, especially in those with high viral burdens.

2. Materials and Methods

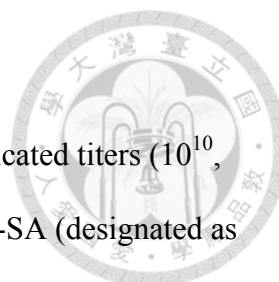


2.1 Animals

Male C57BL/6 mice were purchased from the National Laboratory Animal Breeding and Research Center (Taipei, Taiwan). PD-L1 KO mice were kindly provided by Dr. Lieping Chen (59). All animals were housed in a specific pathogen-free environment in the animal facility of the Institute of Biomedical Sciences, Academia Sinica. All experimental procedures complied with the regulations of the Academia Sinica Institutional Animal Care and Use Committee and the Council of Agriculture Guidebook for the Care and Use of Laboratory Animals.

2.2 Adeno-associated viral (AAV) vectors

The AAV2/8-5'HBV-SD and AAV2/8-3'HBV-SA which contain 5'-HBV and 3'-HBV genome, respectively, were generated and described previously (52). Briefly, plasmid pHBV1.3, containing the 1.3-times overlength HBV genome (genotype D), was split at the CAG/G site between nucleotides 2192 and 2193. A highly conserved synthetic intron was inserted at the split site. Plasmids pAAV5'-HBV-SD and pAAV-3'-HBV-SA were generated by subcloning the two halves of HBV genome were subcloned into the pAAV-MCS vector (Stratagene, La Jolla, CA), which contains the inverted terminal repeat of AAV serotype 2 at both ends. AAV/Empty that contains no transgene served as a negative control. All AAV vectors were generated by the triple transfection method and purified by CsCl sedimentation (58). The physical vector genome (vg) of AAV was measured by quantitative PCR using SYBR Green reaction mix (Roche Diagnostics, Mannheim, Germany) (60).



2.3 AAV injection

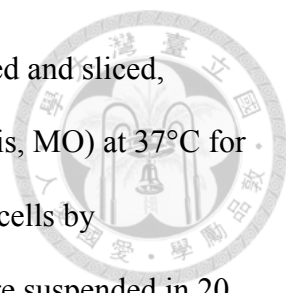
Mice at 6-8 weeks of age were intravenously injected with the indicated titers (10^{10} , 10^{11} , or 10^{12} vg) of both AAV2/8-5'-HBV-SD and AAV2/8/-3'-HBV-SA (designated as AAV/HBV). Mice injected with AAV/Empty of the same titers were used as negative controls.

2.4 Immunization

In vivo electroporation following plasmid injection was performed as previously described (61). Briefly, mice were anesthetized with acepromazine maleate (Fermenta Animal Health Co., Kansas, Mo., USA). Fifty micrograms of plasmid DNA encoding CMV promoter-driven HBsAg, HBcAg, or OVA was injected into each bilateral quadriceps muscles using a disposable insulin syringe with a 27-gauge needle. Immediately after injection, a pair of electrode needles was inserted into the muscle to a depth of 5 mm to encompass the DNA injection sites, and electric pulses were delivered using an electric pulse generator (Electro Square Porator ECM 830; BTX, San Diego, Calif., USA). The shape of the pulse was a square wave. The electrodes consisted of a pair of gold-plated stainless steel needles 5 mm in length and 0.8 mm in diameter with a fixed distance between them of 5 mm. Six pulses of 100 V each were administered to each injection site at a rate of 1 pulse/s, with each pulse being 50 miniseconds in duration. The procedure was repeated once two weeks after the first immunization. In experiments indicated, mice were i.v. injected with 1×10^8 PFU of adenoviral vector expressing pre-S2 envelope protein one week after the second DNA immunization.

2.5 Isolation of splenocytes and intrahepatic lymphocytes

Splenocytes and intrahepatic lymphocytes were isolated on a Percoll density gradient



as described (62). Briefly, the liver was perfused with HBSS, removed and sliced, followed by incubation with collagenase IV (Sigma-Aldrich, St. Louis, MO) at 37°C for 30 min. Intrahepatic lymphocytes were separated from parenchymal cells by centrifugation at 50×g for 5 min. Cells prepared from one mouse were suspended in 20 ml of 33% Percoll gradient solution (GE Healthcare, Piscataway, NJ) and centrifuged at 754×g for 18 min. After treated with red blood cell lysis buffer and washed with PBS, cells were used for IFN- γ ELISPOT and flow cytometric analysis.

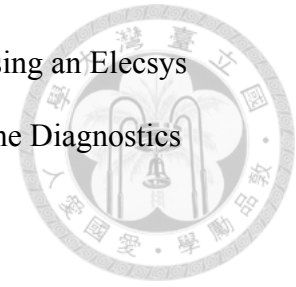
2.6 IFN- γ and TNF- α ELISPOT

CD8 T cells were positively selected from intrahepatic and splenic lymphocytes using mouse CD8a MicroBeads and magnetic separator (Miltenyi Biotec, Bergisch-Gladbach, Germany). Mouse IFN- γ and TNF- α ELISPOT Ready-Set-Go kit (eBioscience, San Diego, CA) was used according to the manufacturer's instruction. Briefly, CD8 T cells (2.5×10^4 to 5×10^5 cells per well) were cocultured with EL4 cells, a murine thymoma cell line derived from C57BL/6 mice, pulsed with 10 $\mu\text{g}/\text{ml}$ of peptides on MultiScreen-IP plates (Millipore, Bedford MA) precoated with α -IFN- γ capture antibody. Three H-2K^b-restricted HBV epitopes, HBS₁₉₀₋₁₉₇, HBS₂₀₈₋₂₁₅, and HBC₉₃₋₁₀₀ were used. The OVA₂₅₇₋₂₆₄ peptide, an H2-K^b-restricted ovalbumin epitope and Con A (2 $\mu\text{g}/\text{ml}$) were used as negative and positive controls, respectively. Spots were developed 18-24 h and detected sequentially with biotinylated antibody against IFN- γ , streptavidin-horseradish peroxidase, and AEC substrates. Spots were counted with AID ELISPOT Reader System with software 5.0 (AID GmbH, Ottobrunn, Germany).

2.7 Serological analysis

Sera samples were collected at different time points post AAV injection. Serological

markers for HBV (HBsAg and α -HBs antibodies) were quantified using an Elecsys Systems electrochemiluminescence kit and a Cobas e analyzer (Roche Diagnostics GmbH, Mannheim, Germany).



2.8 Flow cytometric analysis and fluorescence-activating cell sorting

(FACS)

PD-1 expression on intrahepatic and splenic T lymphocytes was characterized by flow cytometric analysis. Cells were pre-incubated with α -CD16/32 monoclonal antibody (mAb, 2.4G2; ATCC, Manassas, VA) to block nonspecific binding of antibodies to Fc receptors. Cells were then incubated with the following mAbs for 30 min on ice: eFluor[®] 450-conjugated rat α -mouse TCR β (H57-597, eBioscience, San Diego, CA), allophycocyanin (APC)-eFluor[®] 780-conjugated rat α -mouse CD8a (53-6.7, eBioscience, San Diego, CA), phycoerythrin (PE)-conjugated hamster α -mouse PD-1 (J43, eBioscience, San Diego, CA), PE-conjugated rat α -mouse LAG-3 (C9B7W, eBioscience, San Diego, CA), fluorescein isothiocyanate (FITC)-conjugated rat α -mouse 2B4 (eBio244F4, eBioscience, San Diego, CA), Peridinin-Chlorophyll-Protein-Complex (PerCP)-conjugated rat α -mouse Tim-3 (215008, R&D Systems Inc., Minneapolis, MN), and Alexa Fluor 647-conjugated rat α -mouse CD11a (M17/4, Biolegend, San Diego, CA). After wash, cells were stained with fixable viability dye eFluor[®] 506 for 30 min on ice. Cells were analyzed with FACS LSRII (BD Biosciences, San Jose, CA) and FlowJo V.7.2.5 software (Treestar, Ashland, OR). For intracellular cytokine staining, cells were harvested after culture for 6-12 hours in the presence of brefeldin A (Biolegend, San Diego, CA) in U-bottom 96-well plates. After stained with surface marker and viability dye, cells were fixed and permeabilized with fixation/permeabilization kit (eBioscience, San Diego, CA) for 1

hour. The following mAbs were used for cytokine staining: PE-conjugated rat α -mouse IFN- γ (XMG1.2, BD Biosciences, San Jose, CA) and FITC-conjugated rat α -mouse TNF- α (MP6-XT22, eBioscience, San Diego, CA). For FACS, lymphocytes isolated from the liver and the spleen were stained with TCR β , CD8a, and PD-1 as previous described after blocking. 7-amino-actinomycin D (7-AAD, eBioscience, San Diego, CA) was used to rule out dead cells.

2.9 *In vivo* blockade with mAb injection

Mice at 6-8 weeks of age were intraperitoneally injected with 200 μ g of α -LAG-3 mAb (clone C9B7W, BioXCell, West Lebanon, NH) or Rat-IgG isotype control antibody on day -7, -1, 4, 8, 15, 21, 25, 39, 47, and 56. On day 0, treated mice were i.v. injected with 10^{11} vg AAV/HBV.

2.10 Preparation of bone marrow-derived dendritic cells (BMDCs) and *in vitro* adenovirus infection

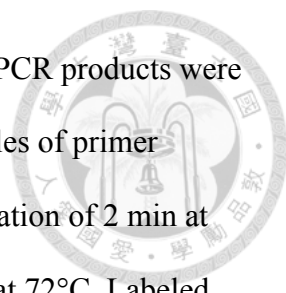
BMDCs were generated following the method reported by Lutz et al (63). In brief, bone marrow cells were isolated from femurs and tibiae, and cultured on Petri dish with RPMI containing 10% FBS, 50 μ M b-ME, and 200 U/ml of GM-CSF. Fresh GM-CSF-containing medium was replenished on day 3, 6, and 8. On day 10, suspended cells were collected and infected with 50 MOI of adenoviral vectors expressing either full-length HBV, pre-S2 envelope protein, HBcAg, by centrifugation at 2000 \times g, 37 $^{\circ}$ C for 2 hours (64). After wash twice with PBS, BMDCs were cultured in RPMI containing 100 U/ml of GM-CSF for 24 hours before subjected to further stimulation.

2.11 *In vitro* T-cell expansion

CD8 T cells were expanded *in vitro* with protocols modified from previous studies (23, 65). Briefly, Sorted CD8 T cells (2×10^4 per well) were co-cultured in U-bottom 96-well plates with LPS-primed BMDCs (2×10^4 per well) that were pulsed with overlapping peptide pools. Naïve splenocytes (2×10^5 per well) that were previously irradiated with 45 Gy γ -radiation were added as feeder cells. The culture medium (RPMI with 10% FBS, 50 μ M β -ME) contains interleukin-7 (IL-7, 5 ng/ml), IL-12 (100 pg/ml), IL-15 (1 ng/ml), and Dynabeads coated with α -CD3 plus α -CD28 mAbs (8×10^4 per well). IL-2 (100 U/ml) was added on day 4 of culture. On day 10, 150 μ l of culture medium was aspirated and peptide-pulsed irradiated naïve splenocytes were added along with 100U/ml of IL-2 for a second round of expansion. On day 20, all expanded cells were subjected to TNF- α ELISPOT.

2.12 T cell receptor (TCR) repertoire spectratype analysis

To analyze the TCR V β transcript size patterns, cDNA samples were amplified using a TCR C β (TCR β -chain constant region)-specific primer and a set of TCR V β (TCR β -chain variable region)-specific primers (66). Detail sequences are described in Table 2. Sorted cells were subjected to RNA extraction by RNeasy Mini kit (Qiagen, Hilden, Germany) and reverse transcription by Transcriptor Reverse Transcriptase (Roche, Diagnostics, Mannheim, Germany). PCR was performed in a total volume of 12.5 μ l containing 0.1 μ l FastStart Taq DNA polymerase (5 U/ μ l) (Roche Diagnostics, Mannheim, Germany), 1.25 μ l 10 \times reaction buffer, 1 μ l dNTPs (2.5 mM), 0.75 μ l MgCl₂ (25 mM), 1 μ l forward and reverse primers (5 mM) and 1.25 μ l cDNA. After an initial denaturation step of 5 minutes at 95°C, the reactions were subjected to 45 cycles of polymerase chain reaction (PCR; 30 seconds at 95°C, 30 seconds at 60°C, 45 seconds



at 72°C) followed by a final elongation step for 10 minutes at 72°C. PCR products were then labeled with C β -carboxyfluorescein (C β -FAM) primer by 5 cycles of primer extension. The primer extension conditions include an initial denaturation of 2 min at 95°C and 5 PCR cycles of 2 min at 95°C, 2 min at 60°C and 20 min at 72°C. Labeled PCR products were mixed with the cocktail of 10 μ l deionized formamide and GeneScan-500 LIZ size standard (Applied Biosystems, Foster City, CA) and cDNA-fragment length were analyzed with ABI 3700 Analyzer (Applied Biosystems, Foster City, CA) and PeakScanner Analysis Software 1.0 (Applied Biosystems, Foster City, CA) according to the manufacturer's protocol.

2.13 Statistics

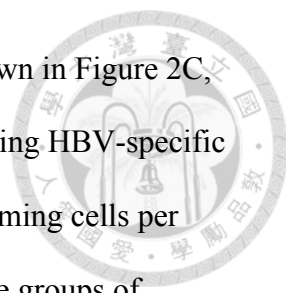
The unpaired Student *t* test was used for statistic analyses. Results were regarded as significant if the two-tailed *p* value was ≤ 0.05 .

3. Results



3.1 Negative Effects of Viral Loads on The Function of HBV-Specific CD8 T Cells

As reported in clinical studies, the viral titers of HBV in chronic carriers correlate *ex vivo* to the numbers and functions of specific CD8 T cells (23). To examine the direct effect of viral loads on the functions of HBV-specific CD8 T cells, we infected C57BL/6 mice with 10^{10} (low), 10^{11} (intermediate), or 10^{12} (hi) vg of AAV/HBV. Infection with these doses of AAV/HBV established persistent expressions of HBsAg, which is detected 6 months p.i. (Figure 1). To gain insight into the functions of HBV-specific CD8 T cells, we treated infected mice at week 2 p.i. with therapeutic vaccination consisting of twice immunization with plasmid DNA encoding HBsAg followed by a booster of adenoviral vector expressing pre-S2 envelope protein. As shown in Figure 2, the levels of serum HBsAg correlated to the viral titers at week 2 p.i. ($5.3 \pm 1.6 \times 10^3$, $5.2 \pm 2.4 \times 10^4$, and $9.7 \pm 0.6 \times 10^4$ IU/ml for low, intermediate, and high viral load groups, respectively). After vaccination, shown in Figure 2A, we observed approximately 50% significant reduction of HBsAg in low and intermediate viral load groups ($2.9 \pm 1.1 \times 10^3$ and $2.7 \pm 0.8 \times 10^4$ IU/ml, $p = 0.049$ and 0.031 , respectively), whereas the level of HBsAg in mice with high viral load reduced only slightly ($8.2 \pm 1.2 \times 10^4$ IU/ml, $p = 0.024$). It is noteworthy that anti-HBs antibodies were detectable in none of the groups of different viral loads (data not shown), suggesting therapeutic vaccine alone was not sufficient to eliminate chronic HBV infection even in the low viral load group. The functions of intrahepatic CD8 T cells at one week after vaccination, however, were restored more efficiently in low viral load group, resulting in 3.1- and 5.1-fold greater numbers of IFN- γ spot-forming cells than that in the groups



of intermediate and high, respectively (Figure 2B). Consistently, shown in Figure 2C, therapeutic vaccination induced the greatest number of IFN- γ producing HBV-specific CD8 T cells in the spleens of low viral load group (273 ± 17 spot-forming cells per million CD8 T cells), which was significantly higher than those in the groups of intermediate (175 ± 22 , $p = 0.002$) and high (27.5 ± 6.6 , $p = 0.0002$). These data revealed a viral load-dependent tolerance of HBV-specific CD8 T cells in this mouse model of chronic HBV infection.

3.2 Intrahepatic T cells from mice with high viral loads expressed higher levels of inhibitory receptors, especially PD-1

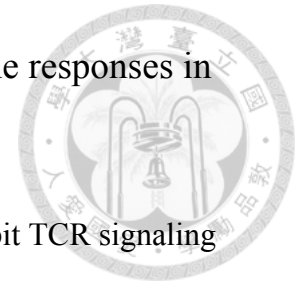
To dissect the mechanisms of HBV-specific immune tolerance in varying degrees, we analyzed the phenotypic profiles of CD8 T cells in the liver and spleen of mice infected with low, intermediate, and high viral loads. After 4 months of AAV/HBV infection, intrahepatic CD8 T cells expressed several inhibitory receptors, including programmed death-1 (PD-1; also known as CD279), 2B4 (CD244), lymphocyte activation gene-3 (LAG-3; CD223). Among these receptors, PD-1 was upregulated with the greatest extent and its expression levels raised as the viral loads increased (Figure 3A). As shown in Figure 3B, in mice with high viral load (10^{12} vg), $49.8 \pm 5.4\%$ of CD8 T cells in the liver expressed PD-1, which is significantly greater than the frequencies of PD-1⁺ CD8 T cells in the liver of intermediate (10^{11} vg) and low (10^{10} vg) viral load groups ($17.6 \pm 3.1\%$ and $2.9 \pm 0.8\%$, respectively). Moreover, intrahepatic CD8 T cells from high viral load mice displayed 2.1- and 6.1-fold higher mean fluorescence intensity (MFI) for PD-1 ($3,097 \pm 518$) in comparison with intermediate and low viral load groups ($1,494 \pm 560$ and 504 ± 59), indicating an reinforced tolerance of intrahepatic CD8 T cells in the context of high viral loads (Figure 3C). In contrast, PD-1 expression

was only slightly upregulated on splenic CD8 T cells (Figure 3A), suggesting a local effect of HBV-induced tolerance in the liver. The induction of PD-1 did not result from the AAV vectors, since it was not observed in mice infected with high dose of AAV/Empty, which contains no transgene (Figure 3A).

Intrahepatic CD8 T cells also overexpressed other inhibitory receptors, such as 2B4 and LAG-3, in a viral load-dependent manner (Figure 4A). Figure 4B shows the percentages of 2B4⁺ cells among total intrahepatic CD8 T cells in mice with different viral loads ($7.7 \pm 3.3\%$, $20.5 \pm 6.0\%$, and $33.5 \pm 1.9\%$ for low, intermediate, and high viral load, respectively). The same trend of upregulation was observed in LAG-3⁺ cells ($4.0 \pm 0.6\%$, $9.0 \pm 2.4\%$, and $28.4 \pm 2.4\%$ for low, intermediate, and high viral load, respectively). The expression levels of 2B4 and LAG-3 were more moderate in comparison with that of PD-1. Upregulation of Tim-3 was only observed on intrahepatic CD8 T cells of high viral load group ($7.2 \pm 0.2\%$). No overexpression of inhibitory receptors on splenic CD8 T cells was detected.

A viral load-dependent PD-1 upregulation was also found on intrahepatic CD4 T cells (Figure 5A). As shown in Figure 5B, the frequency of PD-1⁺ CD4 T cells was the highest in high viral load group ($57.6 \pm 0.8\%$), compared with intermediate group ($31.1 \pm 5.1\%$) and low group ($14.9 \pm 0.7\%$). Surprisingly, splenic CD4 T cells expressed PD-1, whose expression levels were independent on viral loads. In AAV/Empty mice, the expression of PD-1 was also found on splenic CD4 T cells but not on CD8 T cells (data not shown), suggesting an effect irrelevant to HBV. The upregulation of other inhibitory receptors were not observed on both intrahepatic and splenic CD4 T cells. These data indicate that exhausted phenotypes of CD8 and CD4 T cells were induced locally by AAV/HBV infection in a manner dependent on viral loads.

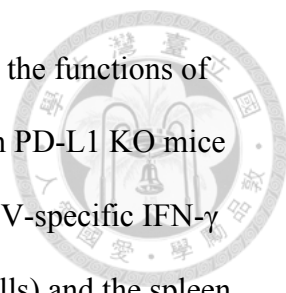
3.3 The reduction of viral antigens and ameliorated immune responses in the absence of PD-1:PD-L1 interaction



Upon engagement to its ligands, PD-1 generated signals that inhibit TCR signaling and subsequent activation of T cells (7). To investigate the role of PD-1 signaling in regulating HBV-specific immunity in this mouse model of HBV infection, we compared the serological and immunological results of WT mice with PD-L1 KO mice, which lack B7-H1, the major ligand of PD-1. After 1 week of infection with 10^{12} vg of AAV/HBV, the level of HBsAg in the serum of PD-L1 KO mice was comparable to that of WT mice (Figure 6A). However, compared to their WT littermates, KO mice showed a significant 11.8-fold reduction of HBsAg at week 2 p.i. As shown in Figure 6B to D, the reduction was concomitant with the observation of more potent IFN- γ production by HBV-specific CD8 T cells from both the liver and spleen of KO mice (1,050 and 385 ± 21 spot-forming cells per million CD8 T cells), in comparison with WT mice (416 and 89 ± 25 spot-forming cells per million CD8 T cells), suggesting the important effect of PD-1:PD-L1 interaction on the regulation of HBV-specific immunity in the early stage of infection.

3.4 Loss of viral control and HBV-specific responses of CD8 T cells in high viral load mice even in the absence of PD-1:PD-L1 interaction

In order to determine the effect of PD-1 signaling on immune tolerance to HBV in the context of different viral loads, we use low, intermediate, and high titers of AAV/HBV to infect WT and PD-L1 KO mice. Serum HBsAg showed comparable levels within the same viral load group at the first week after infection, regardless of deficiency of PD-L1 (data not shown). One week later, the HBsAg levels decreased in KO mice of all viral



load groups (Figure 7). In this early phase of infection (2 weeks p.i.), the functions of HBV-specific CD8 T cells had positive correlation with viral loads in PD-L1 KO mice (Figure 8). In mice infected with high viral loads, the numbers of HBV-specific IFN- γ spot-forming cells were the greatest in the liver (940 spot-forming cells) and the spleen (480 ± 42 spot-forming cells), compared with mice with intermediate and low viral loads.

Nonetheless, in the late phase of infection (week 8 p.i.), the control of viral antigen levels was lost in high viral load mice (Figure 9A to C). The antigen level of KO mice infected with high viral load elevated to the comparable level of WT mice ($9.3 \pm 3.0 \times 10^4$ vs. $7.5 \pm 2.5 \times 10^4$ IU/ml, $p = 0.2$), and this restoration of HBsAg was incomplete in KO mice with intermediate viral loads, whose HBsAg level remained 58% to that of WT mice of intermediate group ($1.5 \pm 0.8 \times 10^4$ vs. $2.7 \pm 0.7 \times 10^4$ IU/ml, $p = 0.04$). The HBsAg level did not rebound in KO mice infected with low viral load at week 8 p.i. ($3.4 \pm 6.0 \times 10^2$ vs. $3.3 \pm 0.9 \times 10^3$ IU/ml, $p = 0.00005$).

Consistent to the observation of viral control, the IFN- γ -secreting HBV-specific CD8 T cells were most numerous in the liver of low-viral load-infected PD-L1 KO mice when compared to intermediate- and high-viral loads (11,360 vs. 2,400 and 2,240 spot-forming cells per million CD8 T cells, Figure 9D and F). The specific CD8 T cells in the spleen of KO mice with low viral load also displayed stronger responses in comparison with mice with intermediate and high loads ($2,346 \pm 164$ vs. 953 ± 41 and 775 ± 16 spot-forming cells per million CD8 T cells). These data indicate that lack of PD-1 signaling is not sufficient to control the viremia and maintain functional specific CD8 T cells in the context of high viral load, suggesting PD-1 partially contributes to the immune tolerance.

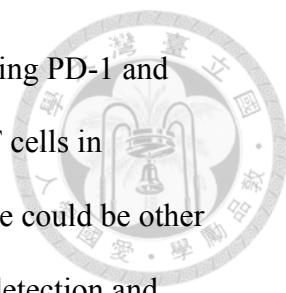
3.5 Blockade of LAG-3 accelerated the reduction of serum HBsAg in PD-L1 KO mice



For further investigation of other factors regulate the establishment of immune tolerance to HBV, we treated WT and PD-L1 KO mice with commercially available α -LAG-3 monoclonal antibody (mAb) to examine the inhibitory effect of LAG-3, one of the potential targets that were overexpressed on intrahepatic CD8 T cells in this model. Mice were intraperitoneally injected with 200 μ g α -LAG-3 mAb or Rat-IgG isotype approximately once a week, starting at one week before infection of AAV/HBV (10^{11} vg). As shown in Figure 10, the first significant reduction of serum HBsAg was observed on day 14 p.i. in PD-L1 KO mice treated with α -LAG-3 mAb (2.5×10^5 IU/ml), compared to day 7 p.i. (6.3×10^5 IU/ml; 2.5-fold reduction, $p = 0.005$). The levels of HBsAg of isotype treated KO mice reduced secondly at day 25 p.i. (7.4×10^4 IU/ml), compared to day 14 p.i. (5.8×10^5 IU/ml; 7.9 fold-reduction, $p = 0.008$). A later reduction was detected in WT mice treated with α -LAG-3 mAb at day 37 p.i. (2.8×10^5 IU/ml), compared to day 25 p.i. (5.0×10^5 IU/ml; 1.8-fold reduction, $p = 0.02$). There is no reduction observed in WT mice treated with isotype control. The HBsAg levels at week 8 p.i. maintained $\sim 50\%$ of the first week after infection in all groups except WT-isotype group. The result suggests a synergistic effect of PD-1 and LAG-3 on the acceleration of viral suppression. However, there is no difference in terms of the suppression level of HBsAg at the late stage of infection.

3.6 Identification of H-2K^b-restricted epitopes of HBsAg and HBcAg

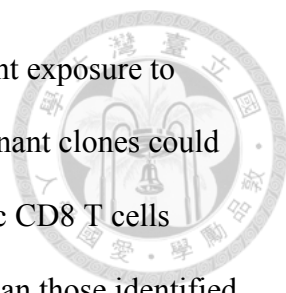
Since the inhibitory receptors on intrahepatic CD8 T cells were only overexpress in AAV/HBV-infected mice but not in AAV/Empty-infected mice, the PD-1⁺ CD8 T cells are reasonably assumed to be specific to HBV. A desired approach to demonstrate the



HBV specificity of PD-1⁺ CD8 T cells is flow cytometric analysis using PD-1 and tetramer staining. However, we were unable to detect specific CD8 T cells in AAV/HBV-infected mice using HBs₁₉₀₋₁₉₇-pentamer, suggesting there could be other clones of HBV-specific CD8 T cells. In order to gain access to the detection and analysis of other clones of HBV-specific CD8 T cells, we screen the sequences of HBsAg and HBcAg to identify all the dominant H-2K^b-restricted epitopes using overlapping peptides that span the whole sequences of HBsAg and HBcAg (Table 1). After immunized with plasmid DNA encoding HBsAg and HBcAg, C57BL/6 were sacrificed and splenic CD8 T cells were subjected to IFN- γ ELISPOT. EL4 cells pulsed with overlapping peptide pools were used to stimulate effector CD8 T cells of immunized mice. Three peptide pools of HBsAg (S31-40, S61-70, and S71-76) and one pool of HBcAg (C21-30) showed positive responses (Figure 11A and B), indicating that these pools contain H-2K^b-restricted epitopes which were recognized by HBV-specific CD8 T cells from immunized mice. A second round of screening was performed using individual peptides from the 4 positive pools discovered in the last IFN- γ ELISPOT. As shown in Figure 11C and D, we found 6 individual peptides that were recognizable by HBV-specific CD8 T cells. Consistent with previous studies (67-69), these individual peptides contain 3 H-2K^b-restricted epitopes: HBs₁₉₀₋₁₉₇ in S70 and S71; HBs₂₀₈₋₂₁₅ in S74 and S75; HBc₉₃₋₁₀₀ in C14 and C15 (labeled in Table 1). HBs₂₀₈₋₂₁₅- and HBc₉₃₋₁₀₀-specific CD8 T cells should be detected with functional tetramer/pentamer in the future.

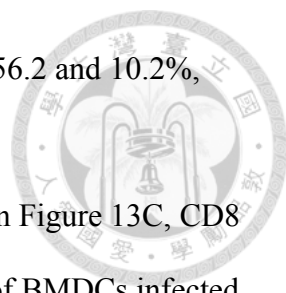
3.7 Detection of subdominant clones of HBV-specific CD8 T cells which recognize other HBV epitopes during chronic infection

Evidences have been shown that dominant clones of virus-specific CD8 T cells can



be subjected to apoptosis that leads to clonal deletion during persistent exposure to cognate antigens in chronic viral infection (70). As a result, subdominant clones could become dominant ones in the late phase of infection. The intrahepatic CD8 T cells overexpressing PD-1 therefore may recognize HBV epitopes other than those identified by a method of immunization (Figure 11). To address whether these PD-1⁺ CD8 T cells are reactive to other epitopes, we isolated intrahepatic lymphocytes from AAV/HBV-infected mice (10¹¹ vg, 12 months p.i.) and stimulated them with EL4 cells pulsed with overlapping peptide pools. The productions of IFN- γ and TNF- α by intrahepatic CD8 T cells were detected by flow cytometric analysis after intracellular cytokine staining, and meanwhile the expression of PD-1 was examined. The frequency of PD-1⁺ expression on intrahepatic CD8 T cells was 33% (data not shown). However, there was no significant production of effector cytokines by total intrahepatic CD8 T cells (both PD-1⁺ and PD-1⁻) after co-culturing with HBV epitope-presenting EL4 cells, compared to control groups of irrelevant epitope (OVA) and EL4 cells alone (Med). Because of exhausted status, these CD8 T cells could lose effector functions upon recognizing cognate epitopes. Thus, a more potent stimulation may be required to activate these CD8 T cells by professional antigen-presenting cells (APCs).

We next test this approach with bone marrow-derived dendritic cells (BMDCs) from PD-L1 KO mice and *in vitro* infected BMDCs using adenoviral vectors expressing either full-length of HBV (Ad-HBV), pre-S2 envelope protein (Ad-mS), or core antigen (Ad-C). The infection of adenovirus resulted in the activation of BMDCs, as the expression of CD80, CD86, and CD40 were highly induced after infection. Mice infected with 10¹² vg AAV/HBV for 6 weeks were sacrificed. After CD8 T cell enrichment from the liver and the spleen, intrahepatic and splenic CD8 T cells were sorted by fluorescence-activating cell sorting (FACS) after PD-1 staining (Figure 13A).

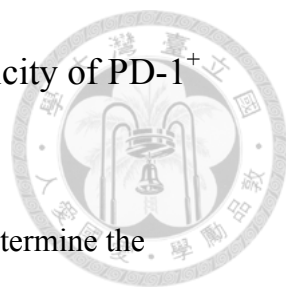


The PD-1 expressions on intrahepatic and splenic CD8 T cells were 56.2 and 10.2%, respectively (Figure 13B). Sorted CD8 T cells were co-cultured with adenovirus-infected BMDCs that express HBV epitopes. As shown in Figure 13C, CD8 T cells from immunized mice (DDA) were activated by stimulation of BMDCs infected by Ad-HBV, Ad-mS, and Ad-C. The degrees of activation were more intense than stimulation by BMDCs infected by adenovirus expressing luciferase (Ad-Luc, negative control), indicating BMDCs infected by Ad-HBV, Ad-mS, and Ad-C were capable of eliciting activation of HBV-specific CD8 T cells. After co-culture, the sorted PD-1⁻ and PD-1⁺ CD8 T cells showed no positive responses to HBV-specific stimulation when compared to Ad-Luc control, suggesting the stimulation by professional APCs may not be sufficient to activate the exhausted T cells.

In clinical studies, dysfunctional CD8 T cells from patients of chronic infection or cancer were *in vitro* expanded with the stimulation of epitopes prior to functional assay (23, 65, 71). The sorted PD-1⁻ and PD-1⁺ intrahepatic CD8 T cells used in Figure 13 were *in vitro* expanded by co-culture with BMDCs irradiated naïve splenocytes pulsed with overlapping peptide pools. After 2 rounds of *in vitro* expansion, all expanded cells were subjected to TNF- α ELISPOT, in which peptide-pulsed EL4 cells were used to stimulate the expanded CD8 T cells. Figure 14 shows that a positive response was detected in PD-1⁺ CD8 T cells stimulated with peptide pool S51-60 in TNF- α ELISPOT. This response was not observed in PD-1⁻ CD8 T cells stimulated with the same peptide pool. The data suggests that the PD-1 expressing CD8 T cells consist of HBV-specific CD8 T cells.

3.8 Alternative approaches to demonstrate the HBV-specificity of PD-1⁺

CD8 T cells



In addition to functional assays, alternative methods are used to determine the pathogen-specificity of T cells. Antigen-specific CD8 T cells express higher amounts of CD11a and the upregulation of CD11a results from exposure to cognate antigens but not inflammation (72). In infection models that lack the information about MHC I-restricted epitopes, the antigen-experienced CD8 T cells with a portrait of CD11a^{hi} were defined as pathogen-specific CD8 T cells (18). In AAV/HBV infected mice, CD11a^{hi} CD8 T cells were detected in the liver and the frequencies of these antigen-experienced CD8 T cells were correlated to the viral loads and antigen levels (Figure 15A and C). The correlation between viral loads and the frequencies of CD11a^{hi} CD8 T cells in the spleen was also observed (data not shown). All PD-1⁺ CD8 T cells expressed high level of CD11a (Figure 15B). However, a proportion of CD11a^{hi} CD8 T cells was PD-1 negative, suggesting some antigen-experienced CD8 T cells did not overexpress PD-1.

HBV-specific CD8 T cells are assumed to be derived from oligoclonal expansion of naïve T cells. As a result, oligoclonal expansion of T cells is supposed to be detected in PD-1⁺ CD8 T cells. To prove this, we sorted intrahepatic CD8 T cells by FACS after PD-1 staining and analyze the lengths of CDR3 in TCR β cDNA by PCR with primers specific for TCR β variable regions after RNA extraction and reverse transcription. The CDR3 lengths of naïve T cells are randomly distributed due to rearrangement of CDR locus, and thus the spectratype of CDR3 of naïve T cells shows a Gaussian distribution. T cell repertoire that undergoes oligoclonal expansion contains more cells with certain length of CDR3, and thus a protruding peak rises in the spectratype profile. As shown in Figure 16, non-Gaussian distributions were observed in 17 out of 20 spectratype profiles (85%) of PD-1⁺ intrahepatic CD8 T cells (labeled with arrows), whereas only 6 profiles

of abnormal distribution (27%) were observed in PD-1⁻ counterpart. These data provide indirect evidences showing the existence of antigen-specificity in PD-1⁺ intrahepatic CD8 T cell, but not in PD-1⁻ ones.



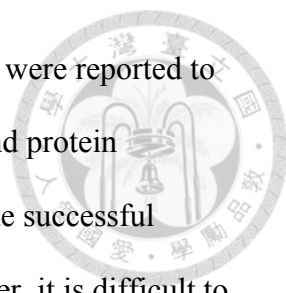
4. Discussion



In summary, our results demonstrated that chronic HBV infection with high levels of viral antigens resulted in upregulation of PD-1 expression and great levels of dysfunction of HBV-specific CD8 T cells. Serum antigen levels in the early phase of infection was reduced in the absence of PD-1:PD-L1 signaling, along with the functional restoration of HBV-specific CD8 T cells. However, impeding the PD-1:PD-L1 inhibitory signal was not sufficient to achieve long-term suppression of HBV in mice infected with high viral loads and the partially restored function of HBV-specific CD8 T cells was unable to eliminate the persistent virus.

4.1 Model advantage

More than 350 millions of people are suffering from persistent HBV infection and in high risks of viral hepatitis-derived liver cirrhosis and hepatocellular carcinoma (73, 74). Although effective prophylaxis vaccinations have immensely reduced the rate of new infection, therapeutic approaches that facilitate the elimination of the cunning virus are still anticipated by chronic carriers, whose immune responses against HBV are found impaired in comparison to acute patients. Because HBV is unable to infect mouse hepatocytes, the lack of suitable mouse models of chronic infection impedes experimental researches for understanding how HBV prevents the induction of antiviral immune responses and establishes persistent infection. HBV-transgenic mice were firstly introduced as a mouse model of chronic carrier for the studies of anti-HBV immunity in chronic infection (48, 49). HBV-specific CD8 T cells are absent in these mice due to central tolerance and have to be generated by other donors and adoptively transferred into the transgenic recipients. Hydrodynamic injection of plasmids or



infection of adenoviral vectors carrying the full-length HBV genome were reported to bypass the viral entry step and achieve long-term HBV replication and protein expression in mouse hepatocytes (50, 51, 75). These approaches made successful models of chronic HBV infection in immunocompetent mice, however, it is difficult to manipulate viral doses in the infected hosts because of the experimental limitations of these models. Using adeno-associated viral vectors as a delivery system, we showed in this report that we are able to control the viral loads in immunocompetent hosts via different sizes of viral inoculum and all of the doses can establish persistent expression of HBV proteins (Figure 1). This allows us to address the effects of different viral loads on immune tolerance to HBV in a system with homogenous host genetics, viral genotypes, and infection durations. For a comprehensive study of HBV-specific cellular immune responses, we screened HBV epitopes in the context of H2-Kb by overlapping peptide and identified 3 dominant epitopes of HBsAg and HBcAg that were previously reported (Figure 11) (67-69). We therefore focused on the functions and phenotypes of CD8 T cells recognizing these three HBV epitopes during persistent HBV infection.

4.2 Tolerance

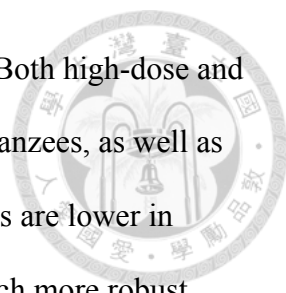
Our AAV/HBV infection model recapitulates several immunological features of chronic viral infections. In chronic viral infections of humans with HIV, HBV, and HCV and of mice with LCMV, virus-specific CD8 T cells are characterized with exhausted phenotypes (1, 3, 76, 77). Virus-specific CD8 T cells show transient function upon stimulation of cognate antigens but acquire functional loss during the progression of chronic infection, including impairment of cytokine production, cytolytic activity, and proliferation. Consistently, in our AAV/HBV infection mouse model we observed a peak of HBs-specific CD8 T cells in the liver and the spleen at week 2 p.i. (early phase

of infection), which became undetectable in later time points. The transient responses against HBV are seldom observed in patients at an early stage of chronic infection. The exhaustion of CD8 T cells was specific to HBV, as the immunization of OVA in AAV/HBV-infected mice generated the same quantity and quality of OVA-specific IFN- γ production from CD8 T cells as compared with that in the control mice.

Interestingly, we observed a higher frequency of HBs-specific CD8 T cells in the liver than in the spleen, which is in line with clinical observations, indicating HBV-specific CD8 T cells are more enriched locally than peripherally (78).

4.3 Dose effect

Clinical studies showed an inverse correlation of viral loads and the antiviral functions of virus-specific CD8 T cells in chronic infections of HIV and HBV (22, 23). However, due to the complexity of clinical samples it is still elusive that whether high viral loads of HBV are the cause or the consequence of CD8 T cell exhaustion. By manipulating the viral doses used for infection, we demonstrated clearly that higher viral loads led to more severe status of immune dysfunction of HBV-specific CD8 T cells. Therapeutic vaccination restored the production of IFN- γ by HBV-specific CD8 T cells to a greater extent in mice with low viral loads, whose serum antigen levels reduced approximately 50% (Figure 2). In contrast, the level of HBsAg in mice with high viral load was slightly reduced (15% reduction). It is noteworthy that there is no elevation of ALT detected after vaccination, suggesting a non-cytolytic control could have contributed to the reduction of viral antigen through production of antiviral cytokines, such as IFN- γ , by HBV-specific CD8 T cells (74). Interestingly, Asabe and colleagues demonstrate that HBV persistency and impaired CD8 T cell functions were observed in chimpanzees inoculated with very low viral titers, attributed to the late

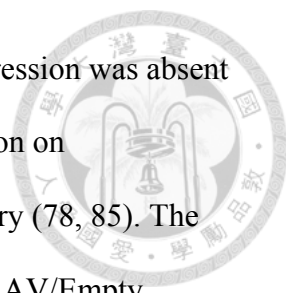


priming of CD4 T cells after 100% of hepatocytes are infected (79). Both high-dose and low-dose inocula of HBV cause high viral burdens in infected chimpanzees, as well as poor responses of intrahepatic CD8 T cells. In contrast, the viral loads are lower in chimpanzees infected with intermediate sizes of viral inocula, in which more robust CD8 T cell responses are found in the liver.

In clinical studies of chronic carriers receiving lamivudine treatments for 1 year, restoration of HBV-specific T cell functions can be extensively observed after dramatic decrease of HBV loads, as a result of suppression of viral replication (80, 81). This phenomenon indicates an effect of viral loads on the inhibition of T cell responses. However, the restoration was only transiently induced and declined 4 months after the starting of treatments, regardless of the sustained viral suppression, suggesting the requirement of other immune stimulations to reinforce and extend the antiviral immunity (82).

4.4 PD-1 expression and other regulatory factors

During persistent infection, exhausted virus-specific CD8 T cells express several inhibitory receptors which generate suppressive signals when ligation with their ligands (4). PD-1, one of the first implicated inhibitory receptors in T cell exhaustion, is highly expressed on virus-specific T cells and recruits SH2-domain containing tyrosine phosphatase 1 (SHP-1) and SHP-2 which inhibit TCR signaling (7). Upregulation of PD-1 is observed on HBV-specific CD8 T cells of chronic carriers and inversely correlated with viral burdens (23, 42, 83). As shown in Figure 3, infection of higher doses of HBV led to not only higher frequencies of PD-1⁺ CD8 T cells but greater degree of PD-1 expression on each CD8 T cells, suggesting the tolerance of CD8 T cells in the liver was reinforced in the context of higher viral loads (84). The results were



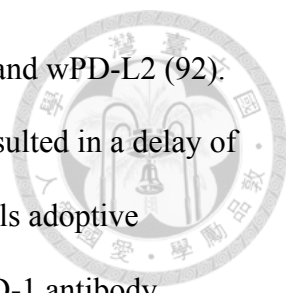
only found in the liver, while the dose-dependent effect of PD-1 expression was absent in the spleen. This is in line with clinical findings that PD-1 expression on HBV-specific CD8 T cells was higher in the liver than in the periphery (78, 85). The induction of PD-1 on intrahepatic CD8 T cells was not observed in AAV/Empty infected mice, indicating a HBV-dependent mechanism of PD-1 induction rather than an AAV-derived effect. Increased PD-1 expression on CD4 T cells was also observed in a dose-dependent manner (Figure 5), implicating a lack of CD4 T cell help which is necessary for the effector functions of HBV-specific CD8 T cells (40, 79, 86). It is controversial whether frequencies of CD4⁺CD25⁺Foxp3⁺ regulatory T cells (Treg cells) is increased in chronic HBV patients and whether the frequencies of Treg cells is correlated with outcome of HBV infection (87). Accumulation of Treg cells was not detected in this model of infection (data not shown), which is different from another model using AAV vector as chronic model of HBV infection (88).

4.5 Blocking PD-1

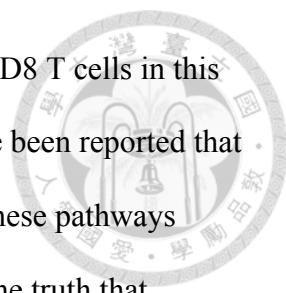
Beginning from the first evidence of the therapeutic effect by blocking PD-1 pathway in LCMV model (5), several independent studies demonstrated that the antiviral functions of virus-specific CD8 T cells from chronic carriers can be restored through the blockade with anti-PD-1 or anti-PD-L1 monoclonal antibodies (6, 23, 89).

Immunotherapy targeting PD-1:PD-L1 interaction has become one of the most promising strategies for rescuing functionally impaired immunity against chronic infections and cancers (15, 90, 91).

The effects of blocking PD-1 pathway on the restoration of HBV-specific T cell functions have been shown in clinical studies (23), as well as in animal models of chronic HBV infection. The proliferation and degranulation of peripheral T cells were



partially enhanced after *in vitro* blockade with Abs against wPD-L1 and wPD-L2 (92). In an *in vivo* study in HBV immune tolerance, blockade of PD-L1 resulted in a delay of the suppression of the antiviral functions of HBV-specific CD8 T cells adoptively transferred into HBV transgenic mice (93). Administration of anti-PD-1 antibody reversed the functional impairment of HBV-specific CD8 T cells and viral persistence in a hydrodynamic injection model, in which the viral burdens are around 10^6 copies per milliliter in the carrier hosts (94). However, large quantities of antigens presented by hepatocytes can lead to a more exhausted state of specific CD8 T cells (95), which renders it unclear whether therapeutic blockade of PD-1:PD-L1 signaling could rescue anti-HBV immunity in the context of high viral loads. To confirm the role of PD-1 signaling in HBV tolerance, we used PD-L1 KO mice in which the major ligand of PD-1 is genetically deprived. Figure 6 showed that lack of PD-1 reinforced the specific functions of HBV-specific CD8 T cells and the levels of HBsAg were reduced in acute phase of infection, a result in line with clinical findings (96, 97). Thereafter, the effect of HBsAg reduction subsided in mice with prolonged exposure to high levels of Ag, while mice with low viral loads maintained the suppression of HBsAg levels (Figure 9A to C). The difference in HBsAg control among the different groups could be attributed to the different degrees of HBV-specific CD8 T cells, which were inversely correlated with the viral load (Figure 9D to G). These results are in keeping with the findings by Shata et al. that high viral loads of HBV cause a more severe status of dysfunction which is more difficult to be rescued (98). It should be noted that although HBV-specific CD8 T cells were more potent in PD-L1 KO mice as compared with those in WT mice (Figure 9F, G vs. Figure 2B, C), these virus-specific T cells were not sufficient to eliminate the persistent virus, particularly in mice with high viral loads, suggesting the existence of regulating factors other than PD-1:PD-L1 pathway. Indeed,

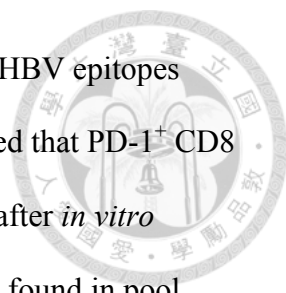


we found several other inhibitory receptors that are upregulated on CD8 T cells in this model of chronic infection (Figure 4). Other suppressive factors have been reported that have negative effects on anti-HBV T cell responses while blocking these pathways restores T cell functions (99-102). Experimental evidences confirm the truth that combinatorial blockades of PD-1 and another inhibitory pathway are more effective to reinforce immunities that eliminate chronic viral infections (14, 17, 103). Besides, combining activation signals with blocking inhibitory pathways increases the functions of intrahepatic T cells of chronic hepatitis B patients (85). Depriving both PD-1 and LAG-3 pathways starting before the infection resulted in accelerated reduction of serum HBsAg level, but was not sufficient to clear the virus (Figure 10). Lack of PD-1 alone had more impact on the decrease of serum antigen level than blocking LAG-3 alone, suggesting a PD-1 pathway is more dominant in regulating T cell tolerance in this model of chronic HBV infection.

4.6 HBV-specificity of PD-1⁺ CD8 T cells

We could not detect comparable amounts of S₁₉₀-pentamer⁺ CD8 T cells in AAV-HBV-infected mice after 4 months p.i. It could result from an altered binding reactivity of these T cells to MHC/peptide complex, which was reported in study of chronic HBV patients (104). Another plausible explanation is that the dominant clone of HBV-specific CD8 T cells has been deleted through apoptosis when exposed to high levels of antigens during chronic viral infection (1, 3, 70, 105).

The alternative ways to demonstrate the antigen-specificity is through functional assays. However, since exhausted CD8 T cells usually lose the antiviral functions, it is a great challenge to use functional approaches to prove the specificity of these T cells to HBV. As a result, we were unable to detect positive responses when stimulating PD-1⁺



CD8 T cells with overlapping peptides and even BMDCs presenting HBV epitopes (Figure 12 and 13). A surprising data shown in Figure 14 was acquired that PD-1⁺ CD8 T cells produced TNF- α in response to overlapping peptides S51-60 after *in vitro* expansion, whereas PD-1⁻ CD8 T cells did not. There was no epitope found in pool S51-60 during epitope screening (Figure 11), indicating a subdominant clone might arise during chronic infection. However, as shown in Figure 15, some antigen-experienced CD8 T cells did not overexpress PD-1, suggesting there are HBV-specific CD8 T cells in PD-1⁻ population. And if PD-1⁻ CD8 T cells were less exhausted, why didn't they react to overlapping peptides? Since the experiment is only done once, it merits further reproducible evidences to confirm this finding.

Finally, indirect evidences that suggest the antigen specificity of intrahepatic PD-1⁺ CD8 T cells were obtained. By gating with surrogate activation marker (CD11a), we illustrated that all intrahepatic PD-1⁺ CD8 T cells possessed the phenotype of antigen-experienced CD8 T cells (Figure 15). In addition, TCR β spectratype analysis showed that there was a higher degree of clonal expansion in PD-1⁺ CD8 T cells than PD-1⁻ ones (Figure 16).

4.7 Conclusion

Our results provide new insights for immunotherapies against chronic HBV infection. First, reducing viral antigens by antiviral therapy, such as nucleot(s)ide analogues or siRNA, could ameliorate the exhaustion of virus-specific T cells and gain benefits to the effect of immunotherapies, as indicated in the clinical reports of lamivudine treatments by Boni and colleagues (80, 81). Second, blocking the inhibitory signals of PD-1:PD-L1 alone may not serve as a sufficient therapeutic approach for activating HBV-specific CD8 T cells, particularly in chronic carriers whose viral

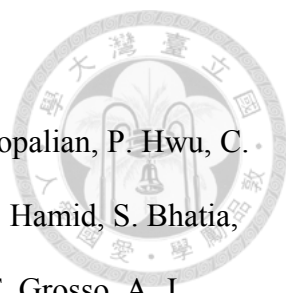
burdens are high. Combinatorial treatments targeting multiple inhibitory pathways and/or activating stimulatory signaling may be required to achieve a better response to clear HBV.

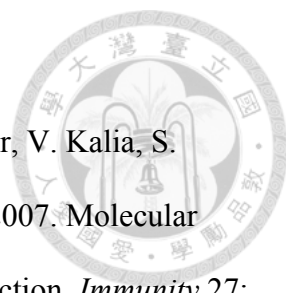



5. References

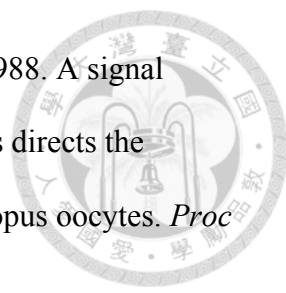


1. Virgin, H. W., E. J. Wherry, and R. Ahmed. 2009. Redefining chronic viral infection. *Cell* 138: 30-50.
2. Ha, S. J., S. N. Mueller, E. J. Wherry, D. L. Barber, R. D. Aubert, A. H. Sharpe, G. J. Freeman, and R. Ahmed. 2008. Enhancing therapeutic vaccination by blocking PD-1-mediated inhibitory signals during chronic infection. *J. Exp. Med.* 205: 543-555.
3. Wherry, E. J. 2011. T cell exhaustion. *Nat. Immunol.* 131: 492-499.
4. Odorizzi, P. M., and E. J. Wherry. 2012. Inhibitory receptors on lymphocytes: insights from infections. *J. Immunol.* 188: 2957-2965.
5. Barber, D. L., E. J. Wherry, D. Masopust, B. Zhu, J. P. Allison, A. H. Sharpe, G. J. Freeman, and R. Ahmed. 2006. Restoring function in exhausted CD8 T cells during chronic viral infection. *Nature* 439: 682-687.
6. Day, C. L., D. E. Kaufmann, P. Kiepiela, J. A. Brown, E. S. Moodley, S. Reddy, E. W. Mackey, J. D. Miller, A. J. Leslie, C. DePierres, Z. Mncube, J. Duraiswamy, B. Zhu, Q. Eichbaum, M. Altfeld, E. J. Wherry, H. M. Coovadia, P. J. Goulder, P. Klenerman, R. Ahmed, G. J. Freeman, and B. D. Walker. 2006. PD-1 expression on HIV-specific T cells is associated with T-cell exhaustion and disease progression. *Nature* 443: 350-354.
7. Keir, M. E., M. J. Butte, G. J. Freeman, and A. H. Sharpe. 2008. PD-1 and its ligands in tolerance and immunity. *Annu. Rev. Immunol.* 26: 677-704.
8. Velu, V., K. Titanji, B. Zhu, S. Husain, A. Pladevega, L. Lai, T. H. Vanderford, L. Chennareddi, G. Silvestri, G. J. Freeman, R. Ahmed, and R. R. Amara. 2009. Enhancing SIV-specific immunity in vivo by PD-1 blockade. *Nature* 458:

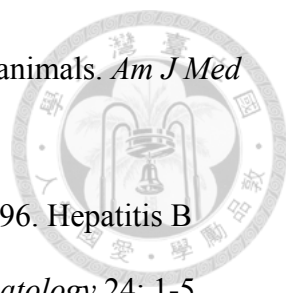
- 
- 206-210.
9. Brahmer, J. R., S. S. Tykodi, L. Q. Chow, W. J. Hwu, S. L. Topalian, P. Hwu, C. G. Drake, L. H. Camacho, J. Kauh, K. Odunsi, H. C. Pitot, O. Hamid, S. Bhatia, R. Martins, K. Eaton, S. Chen, T. M. Salay, S. Alaparthi, J. F. Grosso, A. J. Korman, S. M. Parker, S. Agrawal, S. M. Goldberg, D. M. Pardoll, A. Gupta, and J. M. Wigginton. 2012. Safety and activity of anti-PD-L1 antibody in patients with advanced cancer. *N Engl J Med* 366: 2455-2465.
 10. Hamid, O., C. Robert, A. Daud, F. S. Hodi, W. J. Hwu, R. Kefford, J. D. Wolchok, P. Hersey, R. W. Joseph, J. S. Weber, R. Dronca, T. C. Gangadhar, A. Patnaik, H. Zarour, A. M. Joshua, K. Gergich, J. Elassaiss-Schaap, A. Algazi, C. Mateus, P. Boasberg, P. C. Tumeu, B. Chmielowski, S. W. Ebbinghaus, X. N. Li, S. P. Kang, and A. Ribas. 2013. Safety and Tumor Responses with Lambrolizumab (Anti-PD-1) in Melanoma. *N Engl J Med*.
 11. Topalian, S. L., F. S. Hodi, J. R. Brahmer, S. N. Gettinger, D. C. Smith, D. F. McDermott, J. D. Powderly, R. D. Carvajal, J. A. Sosman, M. B. Atkins, P. D. Leming, D. R. Spigel, S. J. Antonia, L. Horn, C. G. Drake, D. M. Pardoll, L. Chen, W. H. Sharfman, R. A. Anders, J. M. Taube, T. L. McMiller, H. Xu, A. J. Korman, M. Jure-Kunkel, S. Agrawal, D. McDonald, G. D. Kollia, A. Gupta, J. M. Wigginton, and M. Sznol. 2012. Safety, activity, and immune correlates of anti-PD-1 antibody in cancer. *N Engl J Med* 366: 2443-2454.
 12. Wolchok, J. D., H. Kluger, M. K. Callahan, M. A. Postow, N. A. Rizvi, A. M. Lesokhin, N. H. Segal, C. E. Ariyan, R. A. Gordon, K. Reed, M. M. Burke, A. Caldwell, S. A. Kronenberg, B. U. Agunwamba, X. Zhang, I. Lowy, H. D. Inzunza, W. Feely, C. E. Horak, Q. Hong, A. J. Korman, J. M. Wigginton, A. Gupta, and M. Sznol. 2013. Nivolumab plus Ipilimumab in Advanced

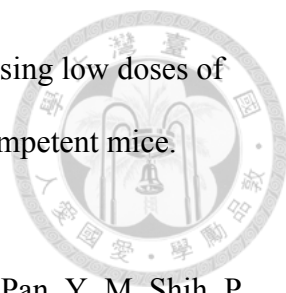
- 
- Melanoma. *N Engl J Med*.
13. Wherry, E. J., S. J. Ha, S. M. Kaech, W. N. Haining, S. Sarkar, V. Kalia, S. Subramaniam, J. N. Blattman, D. L. Barber, and R. Ahmed. 2007. Molecular signature of CD8⁺ T cell exhaustion during chronic viral infection. *Immunity* 27: 670-684.
 14. Jin, H. T., A. C. Anderson, W. G. Tan, E. E. West, S. J. Ha, K. Araki, G. J. Freeman, V. K. Kuchroo, and R. Ahmed. 2010. Cooperation of Tim-3 and PD-1 in CD8 T-cell exhaustion during chronic viral infection. *Proc Natl Acad Sci U S A* 107: 14733-14738.
 15. Youngblood, B., E. J. Wherry, and R. Ahmed. 2012. Acquired transcriptional programming in functional and exhausted virus-specific CD8 T cells. *Curr Opin HIV AIDS* 7: 50-57.
 16. Bengsch, B., B. Seigel, M. Ruhl, J. Timm, M. Kuntz, H. E. Blum, H. Pircher, and R. Thimme. 2010. Coexpression of PD-1, 2B4, CD160 and KLRG1 on exhausted HCV-specific CD8⁺ T cells is linked to antigen recognition and T cell differentiation. *PLoS Pathog* 6: e1000947.
 17. Blackburn, S. D., H. Shin, W. N. Haining, T. Zou, C. J. Workman, A. Polley, M. R. Betts, G. J. Freeman, D. A. Vignali, and E. J. Wherry. 2009. Coregulation of CD8⁺ T cell exhaustion by multiple inhibitory receptors during chronic viral infection. *Nat. Immunol.* 10: 29-37.
 18. Butler, N. S., J. Moebius, L. L. Pewe, B. Traore, O. K. Doumbo, L. T. Tygrett, T. J. Waldschmidt, P. D. Crompton, and J. T. Harty. 2012. Therapeutic blockade of PD-L1 and LAG-3 rapidly clears established blood-stage Plasmodium infection. *Nat. Immunol.* 13: 188-195.
 19. Mueller, S. N., and R. Ahmed. 2009. High antigen levels are the cause of T cell

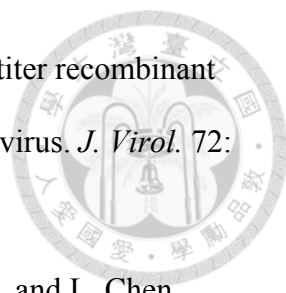
- 
- exhaustion during chronic viral infection. *Proc Natl Acad Sci U S A* 106: 8623-8628.
20. Wherry, E. J., J. N. Blattman, and R. Ahmed. 2005. Low CD8 T-cell proliferative potential and high viral load limit the effectiveness of therapeutic vaccination. *J. Virol.* 79: 8960-8968.
21. West, E. E., B. Youngblood, W. G. Tan, H. T. Jin, K. Araki, G. Alexe, B. T. Konieczny, S. Calpe, G. J. Freeman, C. Terhorst, W. N. Haining, and R. Ahmed. 2011. Tight regulation of memory CD8(+) T cells limits their effectiveness during sustained high viral load. *Immunity* 35: 285-298.
22. Streeck, H., Z. L. Brumme, M. Anastario, K. W. Cohen, J. S. Jolin, A. Meier, C. J. Brumme, E. S. Rosenberg, G. Alter, T. M. Allen, B. D. Walker, and M. Altfeld. 2008. Antigen load and viral sequence diversification determine the functional profile of HIV-1-specific CD8+ T cells. *PLoS Med* 5: e100.
23. Boni, C., P. Fisicaro, C. Valdatta, B. Amadei, P. Di Vincenzo, T. Giuberti, D. Laccabue, A. Zerbini, A. Cavalli, G. Missale, A. Bertoletti, and C. Ferrari. 2007. Characterization of hepatitis B virus (HBV)-specific T-cell dysfunction in chronic HBV infection. *J. Virol.* 81: 4215-4225.
24. Summers, J., and W. S. Mason. 1982. Replication of the genome of a hepatitis B--like virus by reverse transcription of an RNA intermediate. *Cell* 29: 403-415.
25. Chotiyaputta, W., and A. S. Lok. 2009. Hepatitis B virus variants. *Nat Rev Gastroenterol Hepatol* 6: 453-462.
26. Norder, H., A. M. Courouce, P. Coursaget, J. M. Echevarria, S. D. Lee, I. K. Mushahwar, B. H. Robertson, S. Locarnini, and L. O. Magnius. 2004. Genetic diversity of hepatitis B virus strains derived worldwide: genotypes, subgenotypes, and HBsAg subtypes. *Intervirology* 47: 289-309.

- 
27. Standring, D. N., J. H. Ou, F. R. Masiarz, and W. J. Rutter. 1988. A signal peptide encoded within the precore region of hepatitis B virus directs the secretion of a heterogeneous population of e antigens in *Xenopus* oocytes. *Proc Natl Acad Sci U S A* 85: 8405-8409.
28. Schneider, R., D. Fernholz, G. Wildner, and H. Will. 1991. Mechanism, kinetics, and role of duck hepatitis B virus e-antigen expression in vivo. *Virology* 182: 503-512.
29. Chen, H. S., M. C. Kew, W. E. Hornbuckle, B. C. Tennant, P. J. Cote, J. L. Gerin, R. H. Purcell, and R. H. Miller. 1992. The precore gene of the woodchuck hepatitis virus genome is not essential for viral replication in the natural host. *J. Virol.* 66: 5682-5684.
30. Chen, M., M. Sallberg, J. Hughes, J. Jones, L. G. Guidotti, F. V. Chisari, J. N. Billaud, and D. R. Milich. 2005. Immune tolerance split between hepatitis B virus precore and core proteins. *J. Virol.* 79: 3016-3027.
31. Chen, M. T., J. N. Billaud, M. Sallberg, L. G. Guidotti, F. V. Chisari, J. Jones, J. Hughes, and D. R. Milich. 2004. A function of the hepatitis B virus precore protein is to regulate the immune response to the core antigen. *Proc Natl Acad Sci U S A* 101: 14913-14918.
32. Nassal, M. 2008. Hepatitis B viruses: reverse transcription a different way. *Virus Res.* 134: 235-249.
33. Xu, Z., T. S. Yen, L. Wu, C. R. Madden, W. Tan, B. L. Slagle, and J. H. Ou. 2002. Enhancement of hepatitis B virus replication by its X protein in transgenic mice. *J. Virol.* 76: 2579-2584.
34. Feitelson, M. A., H. M. Reis, J. Liu, Z. Lian, and J. Pan. 2005. Hepatitis B virus X antigen (HBxAg) and cell cycle control in chronic infection and

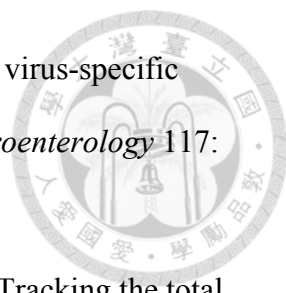
- hepatocarcinogenesis. *Front Biosci* 10: 1558-1572.
35. Yan, H., G. Zhong, G. Xu, W. He, Z. Jing, Z. Gao, Y. Huang, Y. Qi, B. Peng, H. Wang, L. Fu, M. Song, P. Chen, W. Gao, B. Ren, Y. Sun, T. Cai, X. Feng, J. Sui, and W. Li. 2012. Sodium taurocholate cotransporting polypeptide is a functional receptor for human hepatitis B and D virus. *Elife* 1: e00049.
36. Chen, P. J., and T. C. Wu. 2013. One step closer to an experimental infection system for Hepatitis B Virus? --- the identification of sodium taurocholate cotransporting peptide as a viral receptor. *Cell Biosci* 3: 2.
37. McMahon, B. J. 2009. The natural history of chronic hepatitis B virus infection. *Hepatology* 49: S45-55.
38. Horvath, J., and S. P. Raffanti. 1994. Clinical aspects of the interactions between human immunodeficiency virus and the hepatotropic viruses. *Clin. Infect. Dis.* 18: 339-347.
39. Bertoletti, A., and C. Ferrari. 2012. Innate and adaptive immune responses in chronic hepatitis B virus infections: towards restoration of immune control of viral infection. *Gut* 61: 1754-1764.
40. Bertoletti, A., and A. J. Gehring. 2006. The immune response during hepatitis B virus infection. *J. Gen. Virol.* 87: 1439-1449.
41. Rehmann, B., and M. Nascimbeni. 2005. Immunology of hepatitis B virus and hepatitis C virus infection. *Nat. Rev. Immunol.* 5: 215-229.
42. Evans, A., A. Riva, H. Cooksley, S. Phillips, S. Puranik, A. Nathwani, S. Brett, S. Chokshi, and N. V. Naoumov. 2008. Programmed death 1 expression during antiviral treatment of chronic hepatitis B: Impact of hepatitis B e-antigen seroconversion. *Hepatology* 48: 759-769.
43. Barker, L. F., J. E. Maynard, R. H. Purcell, J. H. Hoofnagle, K. R. Berquist, and

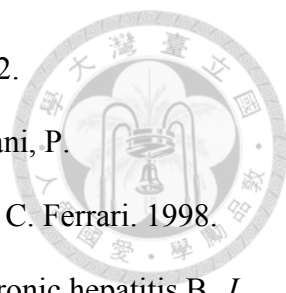
- 
- W. T. London. 1975. Viral hepatitis, type B, in experimental animals. *Am J Med Sci* 270: 189-195.
44. Walter, E., R. Keist, B. Niederost, I. Pult, and H. E. Blum. 1996. Hepatitis B virus infection of tupaia hepatocytes in vitro and in vivo. *Hepatology* 24: 1-5.
45. O'Connell, A. P., M. K. Urban, and W. T. London. 1983. Naturally occurring infection of Pekin duck embryos by duck hepatitis B virus. *Proc Natl Acad Sci U S A* 80: 1703-1706.
46. Millman, I., L. Southam, T. Halbherr, H. Simmons, and C. M. Kang. 1984. Woodchuck hepatitis virus: experimental infection and natural occurrence. *Hepatology* 4: 817-823.
47. Meuleman, P., L. Libbrecht, R. De Vos, B. de Hemptinne, K. Gevaert, J. Vandekerckhove, T. Roskams, and G. Leroux-Roels. 2005. Morphological and biochemical characterization of a human liver in a uPA-SCID mouse chimera. *Hepatology* 41: 847-856.
48. Moriyama, T., S. Guilhot, K. Klopchin, B. Moss, C. A. Pinkert, R. D. Palmiter, R. L. Brinster, O. Kanagawa, and F. V. Chisari. 1990. Immunobiology and pathogenesis of hepatocellular injury in hepatitis B virus transgenic mice. *Science* 248: 361-364.
49. Araki, K., J. Miyazaki, O. Hino, N. Tomita, O. Chisaka, K. Matsubara, and K. Yamamura. 1989. Expression and replication of hepatitis B virus genome in transgenic mice. *Proc Natl Acad Sci U S A* 86: 207-211.
50. Huang, L. R., H. L. Wu, P. J. Chen, and D. S. Chen. 2006. An immunocompetent mouse model for the tolerance of human chronic hepatitis B virus infection. *Proc Natl Acad Sci U S A* 103: 17862-17867.
51. Huang, L. R., Y. A. Gabel, S. Graf, S. Arzberger, C. Kurts, M. Heikenwalder, P.

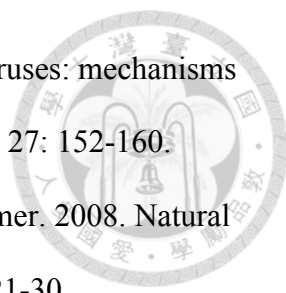
- 
- A. Knolle, and U. Protzer. 2012. Transfer of HBV genomes using low doses of adenovirus vectors leads to persistent infection in immune competent mice. *Gastroenterology* 142: 1447-1450 e1443.
52. Huang, Y. H., C. C. Fang, K. Tsuneyama, H. Y. Chou, W. Y. Pan, Y. M. Shih, P. Y. Wu, Y. Chen, P. S. Leung, M. E. Gershwin, and M. H. Tao. 2011. A murine model of hepatitis B-associated hepatocellular carcinoma generated by adeno-associated virus-mediated gene delivery. *Int. J. Oncol.* 39: 1511-1519.
53. McCaffrey, A. P., P. Fawcett, H. Nakai, R. L. McCaffrey, A. Ehrhardt, T. T. Pham, K. Pandey, H. Xu, S. Feuss, T. A. Storm, and M. A. Kay. 2008. The host response to adenovirus, helper-dependent adenovirus, and adeno-associated virus in mouse liver. *Mol. Ther.* 16: 931-941.
54. Nayak, S., and R. W. Herzog. 2010. Progress and prospects: immune responses to viral vectors. *Gene Ther.* 17: 295-304.
55. Wieland, S., R. Thimme, R. H. Purcell, and F. V. Chisari. 2004. Genomic analysis of the host response to hepatitis B virus infection. *Proc Natl Acad Sci U S A* 101: 6669-6674.
56. Dunn, C., D. Peppas, P. Khanna, G. Nebbia, M. Jones, N. Brendish, R. M. Lascar, D. Brown, R. J. Gilson, R. J. Tedder, G. M. Dusheiko, M. Jacobs, P. Klenerman, and M. K. Maini. 2009. Temporal analysis of early immune responses in patients with acute hepatitis B virus infection. *Gastroenterology* 137: 1289-1300.
57. Duan, D., P. Sharma, J. Yang, Y. Yue, L. Dudus, Y. Zhang, K. J. Fisher, and J. F. Engelhardt. 1998. Circular intermediates of recombinant adeno-associated virus have defined structural characteristics responsible for long-term episomal persistence in muscle tissue. *J. Virol.* 72: 8568-8577.

- 
58. Xiao, X., J. Li, and R. J. Samulski. 1998. Production of high-titer recombinant adeno-associated virus vectors in the absence of helper adenovirus. *J. Virol.* 72: 2224-2232.
59. Dong, H., G. Zhu, K. Tamada, D. B. Flies, J. M. van Deursen, and L. Chen. 2004. B7-H1 determines accumulation and deletion of intrahepatic CD8(+) T lymphocytes. *Immunity* 20: 327-336.
60. Chen, C. C., C. P. Sun, H. I. Ma, C. C. Fang, P. Y. Wu, X. Xiao, and M. H. Tao. 2009. Comparative study of anti-hepatitis B virus RNA interference by double-stranded adeno-associated virus serotypes 7, 8, and 9. *Mol. Ther.* 17: 352-359.
61. Lee, S. C., C. J. Wu, P. Y. Wu, Y. L. Huang, C. W. Wu, and M. H. Tao. 2003. Inhibition of established subcutaneous and metastatic murine tumors by intramuscular electroporation of the interleukin-12 gene. *J. Biomed. Sci.* 10: 73-86.
62. Chang, C. M., C. H. Lo, Y. M. Shih, Y. Chen, P. Y. Wu, K. Tsuneyama, S. R. Roffler, and M. H. Tao. 2010. Treatment of hepatocellular carcinoma with adeno-associated virus encoding interleukin-15 superagonist. *Hum. Gene Ther.* 21: 611-621.
63. Lutz, M. B., N. Kukutsch, A. L. Ogilvie, S. Rossner, F. Koch, N. Romani, and G. Schuler. 1999. An advanced culture method for generating large quantities of highly pure dendritic cells from mouse bone marrow. *J. Immunol. Methods* 223: 77-92.
64. Nishimura, N., Y. Nishioka, T. Shinohara, and S. Sone. 2001. Enhanced efficiency by centrifugal manipulation of adenovirus-mediated interleukin 12 gene transduction into human monocyte-derived dendritic cells. *Hum. Gene*

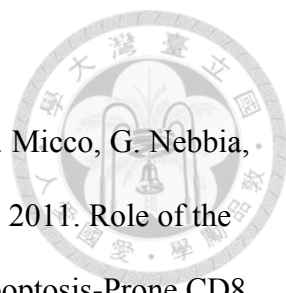
- Ther.* 12: 333-346.
65. Chapuis, A. G., G. B. Ragnarsson, H. N. Nguyen, C. N. Chaney, J. S. Pufnock, T. M. Schmitt, N. Duerkopp, I. M. Roberts, G. L. Pogosov, W. Y. Ho, S. Ochsenreither, M. Wolfl, M. Bar, J. P. Radich, C. Yee, and P. D. Greenberg. 2013. Transferred WT1-reactive CD8⁺ T cells can mediate antileukemic activity and persist in post-transplant patients. *Sci Transl Med* 5: 174ra127.
66. Pannetier, C., M. Cochet, S. Darche, A. Casrouge, M. Zoller, and P. Kourilsky. 1993. The sizes of the CDR3 hypervariable regions of the murine T-cell receptor beta chains vary as a function of the recombined germ-line segments. *Proc Natl Acad Sci U S A* 90: 4319-4323.
67. Kuhober, A., H. P. Pudollek, K. Reifenberg, F. V. Chisari, H. J. Schlicht, J. Reimann, and R. Schirmbeck. 1996. DNA immunization induces antibody and cytotoxic T cell responses to hepatitis B core antigen in H-2b mice. *J. Immunol.* 156: 3687-3695.
68. Schirmbeck, R., W. Bohm, N. Fissolo, K. Melber, and J. Reimann. 2003. Different immunogenicity of H-2 Kb-restricted epitopes in natural variants of the hepatitis B surface antigen. *Eur. J. Immunol.* 33: 2429-2438.
69. Schirmbeck, R., J. Wild, and J. Reimann. 1998. Similar as well as distinct MHC class I-binding peptides are generated by exogenous and endogenous processing of hepatitis B virus surface antigen. *Eur. J. Immunol.* 28: 4149-4161.
70. Zajac, A. J., J. N. Blattman, K. Murali-Krishna, D. J. Sourdive, M. Suresh, J. D. Altman, and R. Ahmed. 1998. Viral immune evasion due to persistence of activated T cells without effector function. *J. Exp. Med.* 188: 2205-2213.
71. Maini, M. K., C. Boni, G. S. Ogg, A. S. King, S. Reignat, C. K. Lee, J. R. Larrubia, G. J. Webster, A. J. McMichael, C. Ferrari, R. Williams, D. Vergani,

- 
- and A. Bertolotti. 1999. Direct ex vivo analysis of hepatitis B virus-specific CD8(+) T cells associated with the control of infection. *Gastroenterology* 117: 1386-1396.
72. Rai, D., N. L. Pham, J. T. Harty, and V. P. Badovinac. 2009. Tracking the total CD8 T cell response to infection reveals substantial discordance in magnitude and kinetics between inbred and outbred hosts. *J. Immunol.* 183: 7672-7681.
73. El-Serag, H. B. 2012. Epidemiology of viral hepatitis and hepatocellular carcinoma. *Gastroenterology* 142: 1264-1273 e1261.
74. Guidotti, L. G., and F. V. Chisari. 2006. Immunobiology and pathogenesis of viral hepatitis. *Annu Rev Pathol* 1: 23-61.
75. Lin, Y. J., L. R. Huang, H. C. Yang, H. T. Tzeng, P. N. Hsu, H. L. Wu, P. J. Chen, and D. S. Chen. 2010. Hepatitis B virus core antigen determines viral persistence in a C57BL/6 mouse model. *Proc Natl Acad Sci U S A* 107: 9340-9345.
76. Fahey, L. M., and D. G. Brooks. 2010. Opposing positive and negative regulation of T cell activity during viral persistence. *Curr. Opin. Immunol.* 22: 348-354.
77. Frebel, H., K. Richter, and A. Oxenius. 2010. How chronic viral infections impact on antigen-specific T-cell responses. *Eur. J. Immunol.* 40: 654-663.
78. Fisicaro, P., C. Valdatta, M. Massari, E. Loggi, E. Biasini, L. Sacchelli, M. C. Cavallo, E. M. Silini, P. Andreone, G. Missale, and C. Ferrari. 2010. Antiviral intrahepatic T-cell responses can be restored by blocking programmed death-1 pathway in chronic hepatitis B. *Gastroenterology* 138: 682-693, 693 e681-684.
79. Asabe, S., S. F. Wieland, P. K. Chattopadhyay, M. Roederer, R. E. Engle, R. H. Purcell, and F. V. Chisari. 2009. The size of the viral inoculum contributes to the

- 
- outcome of hepatitis B virus infection. *J. Virol.* 83: 9652-9662.
80. Boni, C., A. Bertolotti, A. Penna, A. Cavalli, M. Pilli, S. Urbani, P. Scognamiglio, R. Boehme, R. Panebianco, F. Fiaccadori, and C. Ferrari. 1998. Lamivudine treatment can restore T cell responsiveness in chronic hepatitis B. *J. Clin. Invest.* 102: 968-975.
81. Boni, C., A. Penna, G. S. Ogg, A. Bertolotti, M. Pilli, C. Cavallo, A. Cavalli, S. Urbani, R. Boehme, R. Panebianco, F. Fiaccadori, and C. Ferrari. 2001. Lamivudine treatment can overcome cytotoxic T-cell hyporesponsiveness in chronic hepatitis B: new perspectives for immune therapy. *Hepatology* 33: 963-971.
82. Boni, C., A. Penna, A. Bertolotti, V. Lamonaca, I. Rapti, G. Missale, M. Pilli, S. Urbani, A. Cavalli, S. Cerioni, R. Panebianco, J. Jenkins, and C. Ferrari. 2003. Transient restoration of anti-viral T cell responses induced by lamivudine therapy in chronic hepatitis B. *J Hepatol* 39: 595-605.
83. Chen, J., X. M. Wang, X. J. Wu, Y. Wang, H. Zhao, B. Shen, and G. Q. Wang. 2011. Intrahepatic levels of PD-1/PD-L correlate with liver inflammation in chronic hepatitis B. *Inflamm Res* 60: 47-53.
84. Wei, F., S. Zhong, Z. Ma, H. Kong, A. Medvec, R. Ahmed, G. J. Freeman, M. Krogsgaard, and J. L. Riley. 2013. Strength of PD-1 signaling differentially affects T-cell effector functions. *Proc Natl Acad Sci U S A.*
85. Fisicaro, P., C. Valdatta, M. Massari, E. Loggi, L. Ravanetti, S. Urbani, T. Giuberti, A. Cavalli, C. Vandelli, P. Andreone, G. Missale, and C. Ferrari. 2012. Combined blockade of programmed death-1 and activation of CD137 increase responses of human liver T cells against HBV, but not HCV. *Gastroenterology* 143: 1576-1585 e1574.

- 
86. Rehermann, B. 2007. Chronic infections with hepatotropic viruses: mechanisms of impairment of cellular immune responses. *Semin Liver Dis* 27: 152-160.
87. Li, S., E. J. Gowans, C. Chougnet, M. Plebanski, and U. Dittmer. 2008. Natural regulatory T cells and persistent viral infection. *J. Virol.* 82: 21-30.
88. Dion, S., M. Bourguine, O. Godon, F. Levillayer, and M. L. Michel. 2013. Adeno-Associated Virus-Mediated Gene Transfer Leads to Persistent Hepatitis B Virus Replication in Mice Expressing HLA-A2 and HLA-DR1 Molecules. *J. Virol.* 87: 5554-5563.
89. Urbani, S., B. Amadei, D. Tola, M. Massari, S. Schivazappa, G. Missale, and C. Ferrari. 2006. PD-1 expression in acute hepatitis C virus (HCV) infection is associated with HCV-specific CD8 exhaustion. *J. Virol.* 80: 11398-11403.
90. Porichis, F., and D. E. Kaufmann. 2012. Role of PD-1 in HIV pathogenesis and as target for therapy. *Curr HIV/AIDS Rep* 9: 81-90.
91. Sakthivel, P., M. Gereke, and D. Bruder. 2012. Therapeutic intervention in cancer and chronic viral infections: antibody mediated manipulation of PD-1/PD-L1 interaction. *Rev Recent Clin Trials* 7: 10-23.
92. Zhang, E., X. Zhang, J. Liu, B. Wang, Y. Tian, A. D. Kosinska, Z. Ma, Y. Xu, U. Dittmer, M. Roggendorf, D. Yang, and M. Lu. 2011. The expression of PD-1 ligands and their involvement in regulation of T cell functions in acute and chronic woodchuck hepatitis virus infection. *PLoS One* 6: e26196.
93. Maier, H., M. Isogawa, G. J. Freeman, and F. V. Chisari. 2007. PD-1:PD-L1 interactions contribute to the functional suppression of virus-specific CD8⁺ T lymphocytes in the liver. *J. Immunol.* 178: 2714-2720.
94. Tzeng, H. T., H. F. Tsai, H. J. Liao, Y. J. Lin, L. Chen, P. J. Chen, and P. N. Hsu. 2012. PD-1 blockage reverses immune dysfunction and hepatitis B viral

- persistence in a mouse animal model. *PLoS One* 7: e39179.
95. Gehring, A. J., D. Sun, P. T. Kennedy, E. Nolte-'t Hoen, S. G. Lim, S. Wasser, C. Selden, M. K. Maini, D. M. Davis, M. Nassal, and A. Bertoletti. 2007. The level of viral antigen presented by hepatocytes influences CD8 T-cell function. *J. Virol.* 81: 2940-2949.
96. Zhang, Z., B. Jin, J. Y. Zhang, B. Xu, H. Wang, M. Shi, E. J. Wherry, G. K. Lau, and F. S. Wang. 2009. Dynamic decrease in PD-1 expression correlates with HBV-specific memory CD8 T-cell development in acute self-limited hepatitis B patients. *J Hepatol* 50: 1163-1173.
97. Zhang, Z., J. Y. Zhang, E. J. Wherry, B. Jin, B. Xu, Z. S. Zou, S. Y. Zhang, B. S. Li, H. F. Wang, H. Wu, G. K. Lau, Y. X. Fu, and F. S. Wang. 2008. Dynamic programmed death 1 expression by virus-specific CD8 T cells correlates with the outcome of acute hepatitis B. *Gastroenterology* 134: 1938-1949, 1949 e1931-1933.
98. Shata, M. T., W. Pfahler, B. Brotman, D. H. Lee, N. Tricoche, K. Murthy, and A. M. Prince. 2006. Attempted therapeutic immunization in a chimpanzee chronic HBV carrier with a high viral load. *J Med Primatol* 35: 165-171.
99. Cai, G., X. Nie, L. Li, L. Hu, B. Wu, J. Lin, C. Jiang, H. Wang, X. Wang, and Q. Shen. 2013. B and T lymphocyte attenuator is highly expressed on intrahepatic T cells during chronic HBV infection and regulates their function. *J Gastroenterol.*
100. Raziorrouh, B., W. Schraut, T. Gerlach, D. Nowack, N. H. Gruner, A. Ulsenheimer, R. Zachoval, M. Wachtler, M. Spannagl, J. Haas, H. M. Diepolder, and M. C. Jung. 2010. The immunoregulatory role of CD244 in chronic hepatitis B infection and its inhibitory potential on virus-specific CD8+ T-cell function.

- 
- Hepatology* 52: 1934-1947.
101. Schurich, A., P. Khanna, A. R. Lopes, K. J. Han, D. Peppas, L. Micco, G. Nebbia, P. T. Kennedy, A. M. Geretti, G. Dusheiko, and M. K. Maini. 2011. Role of the coinhibitory receptor cytotoxic T lymphocyte antigen-4 on apoptosis-Prone CD8 T cells in persistent hepatitis B virus infection. *Hepatology* 53: 1494-1503.
 102. Wu, W., Y. Shi, S. Li, Y. Zhang, Y. Liu, Y. Wu, and Z. Chen. 2012. Blockade of Tim-3 signaling restores the virus-specific CD8(+) T-cell response in patients with chronic hepatitis B. *Eur. J. Immunol.* 42: 1180-1191.
 103. Brooks, D. G., S. J. Ha, H. Elsaesser, A. H. Sharpe, G. J. Freeman, and M. B. Oldstone. 2008. IL-10 and PD-L1 operate through distinct pathways to suppress T-cell activity during persistent viral infection. *Proc Natl Acad Sci U S A* 105: 20428-20433.
 104. Reignat, S., G. J. Webster, D. Brown, G. S. Ogg, A. King, S. L. Seneviratne, G. Dusheiko, R. Williams, M. K. Maini, and A. Bertoletti. 2002. Escaping high viral load exhaustion: CD8 cells with altered tetramer binding in chronic hepatitis B virus infection. *J. Exp. Med.* 195: 1089-1101.
 105. Homann, D., D. B. McGavern, and M. B. Oldstone. 2004. Visualizing the viral burden: phenotypic and functional alterations of T cells and APCs during persistent infection. *J. Immunol.* 172: 6239-6250.

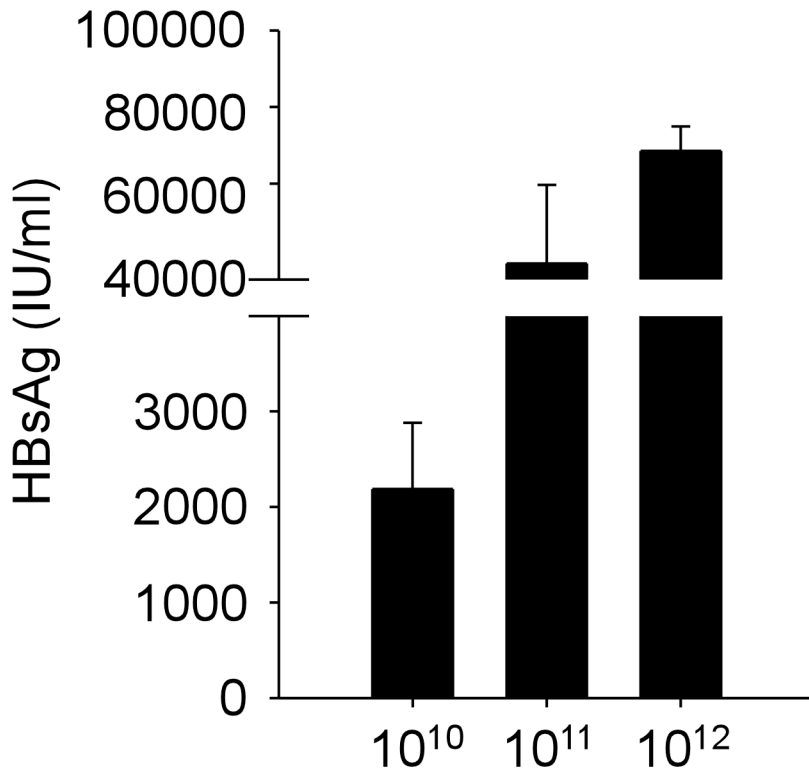


Figure 1. Long-term expression of HBsAg in low, intermediate, and high viral loads

C57BL/6 (B6) mice were i.v. injected with low (10^{10} vg), intermediate (10^{11} vg), or high (10^{12}) viral loads of AAV/HBV. Sera were collected 6 months post-infection (p.i.) for the measurement of HBsAg by electrochemiluminescence. Error bars represent standard deviations (SD).

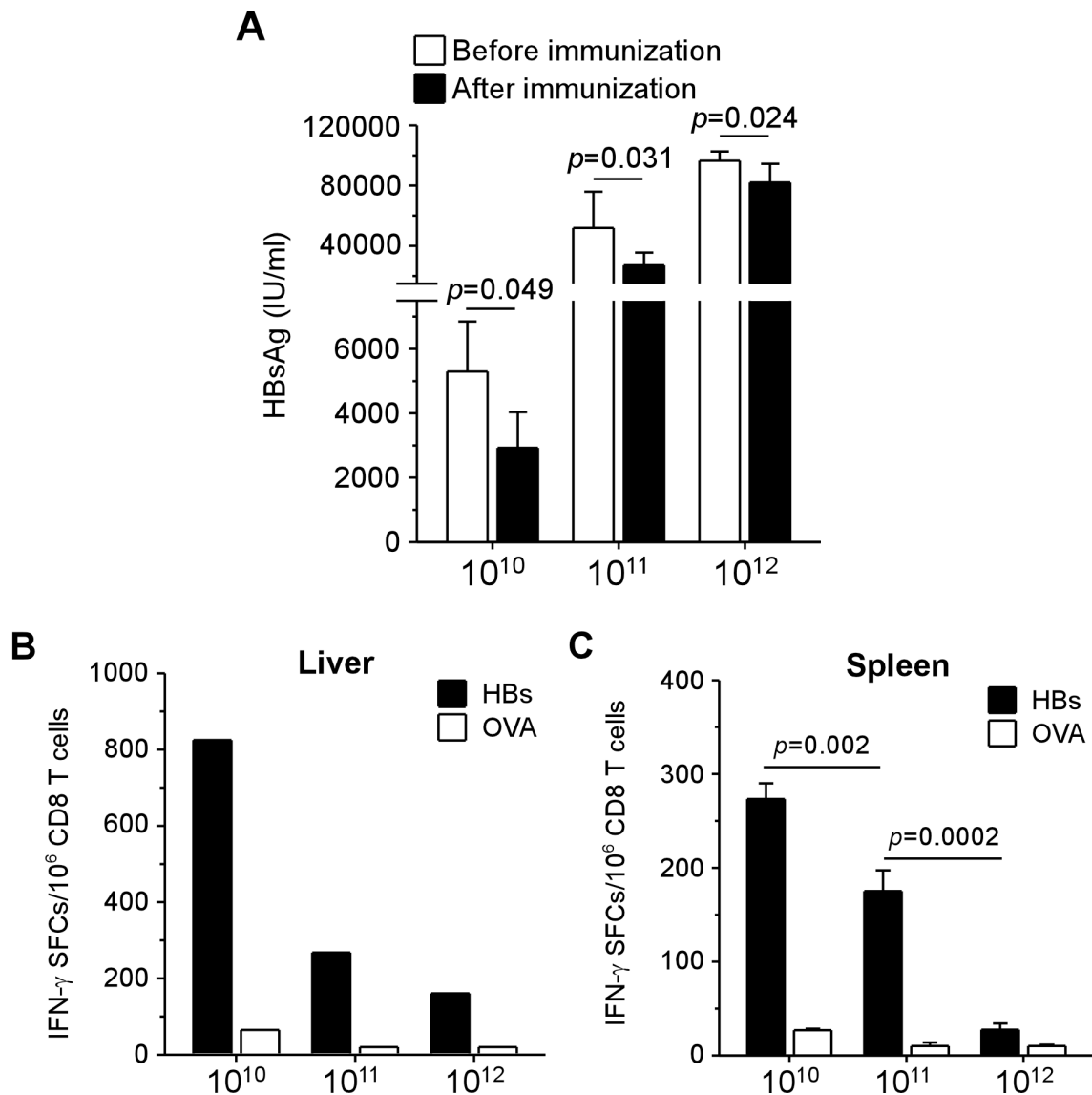
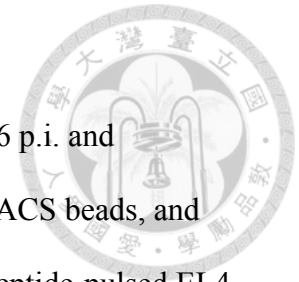


Figure 2. Functional impairment of HBV-specific CD8 T cells depended on viral loads

Mice were infected with different doses (10^{10} , 10^{11} , or 10^{12} vg) of AAV/HBV and treated with therapeutic vaccination. At week 2 p.i., mice were immunized by intramuscular (i.m.) injection with 100 μ g of pHBs plasmid DNA (encoding HBsAg) twice at a two-week interval. One week after the second DNA immunization (week 5 p.i.), mice were i.v. injected with 1×10^8 PFU of adenoviral vector expressing pre-S2 envelope protein. (A) Sera were collected before (week 2 p.i.) and after (week 6 p.i.) the

treatment of therapeutic vaccination for the detection of HBsAg by electrochemiluminescence. (B and C) Mice were sacrificed at week 6 p.i. and intrahepatic and splenic CD8 T cells were isolated, enriched with MACS beads, and subjected to interferon gamma (IFN- γ) ELISPOT assays, in which peptide-pulsed EL4 cells were co-cultured with CD8 T cells for stimulation. Data are representative of three independent experiments with 5 mice per group. Error bars represent SD. SFC, spot-forming cells. HBS, HBS₁₉₀₋₁₉₇ and HBS₂₀₈₋₂₁₅ peptides. OVA, OVA₂₅₇₋₂₆₄ peptide. Med, RPMI 1640 medium.



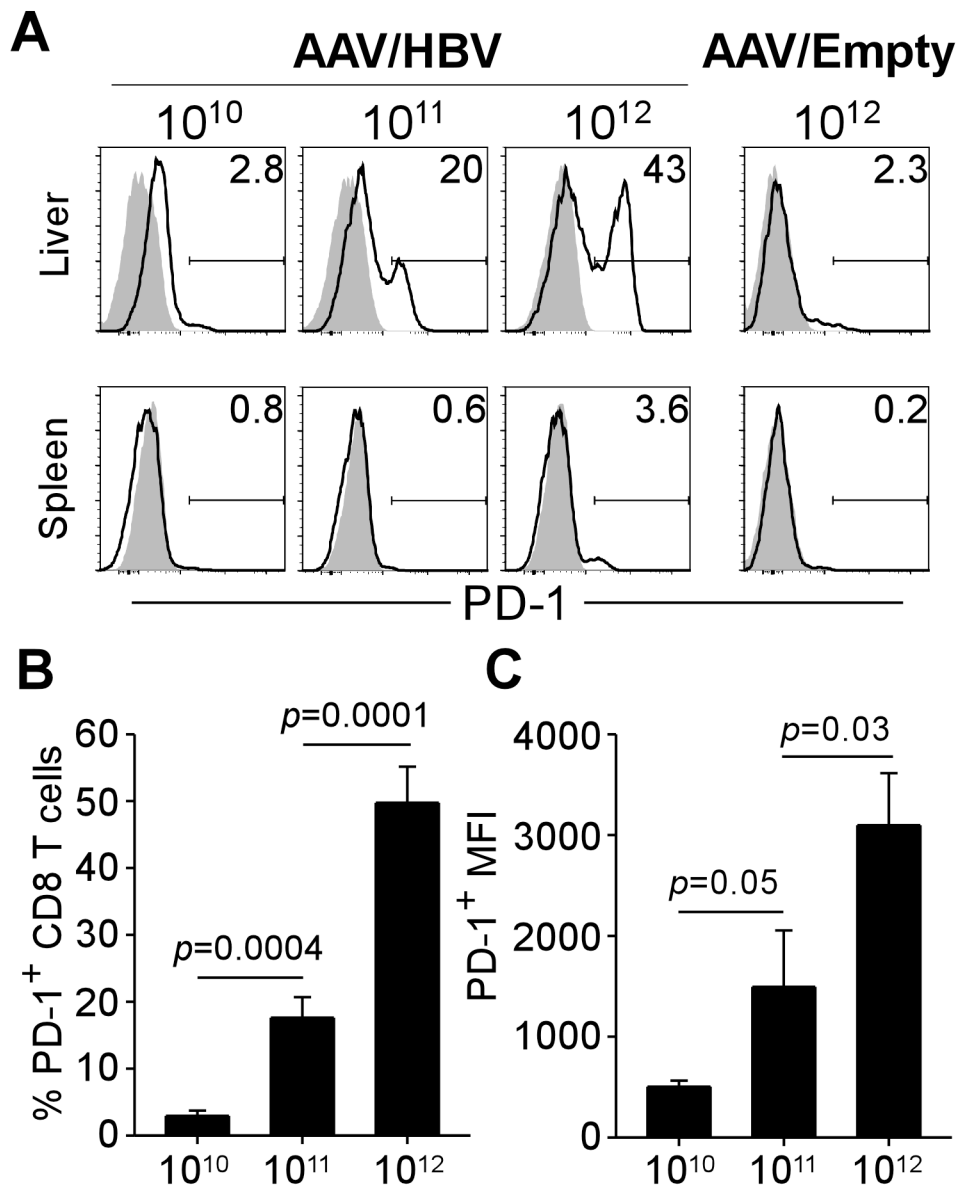


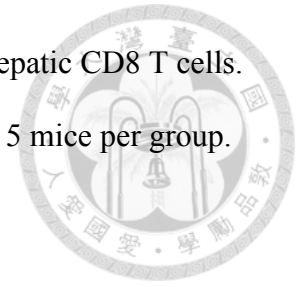
Figure 3. PD-1 expression on intrahepatic CD8 T cells was upregulated in a viral load-dependent manner

Mice were infected with different doses of AAV/HBV and sacrificed 4 months after infection. Lymphocytes in liver and spleen were isolated and analyzed by flow cytometry. The expression of PD-1 was evaluated after gating on viable TCR β ⁺CD8⁺ cells. AAV/Empty served as a negative control. (A) The expression levels of PD-1 on intrahepatic and splenic CD8 T cells. (B) Percentages of PD-1⁺ cells in total intrahepatic

CD8 T cells. (C) Mean fluorescence intensity (MFI) of PD-1⁺ intrahepatic CD8 T cells.

Data were representative of three independent experiments with 3 to 5 mice per group.

Error bars represent SEM.



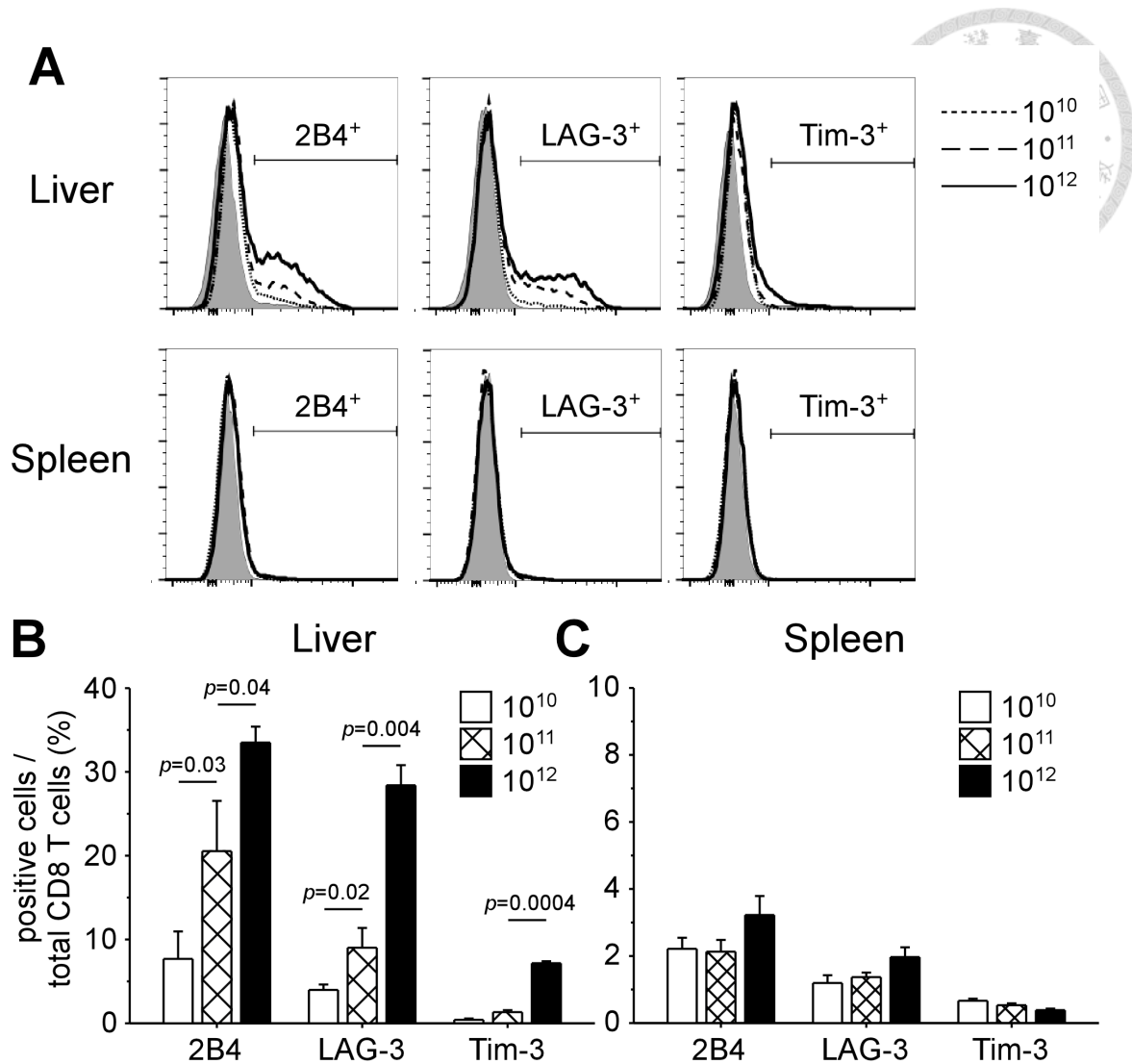


Figure 4. Expression of 2B4 and LAG-3 on intrahepatic CD8 T cells increased with greater extents during infection of higher viral loads

Mice were infected with different doses of AAV/HBV and sacrificed 4 months after infection. Lymphocytes in liver and spleen were isolated and analyzed by flow cytometry. The expressions of 2B4, LAG-3, and Tim-3 were evaluated after gating on viable TCRβ⁺CD8⁺ cells. (A) Representative data of 2B4, LAG-3, and Tim-3 expression on CD8 T cells in the liver and the spleen of mice infected with different loads of AAV/HBV. (B and C) Summary results of 2B4, LAG-3, and Tim-3 expression on intrahepatic and splenic CD8 T cells. Data were representative of three independent experiments with 3 to 5 mice per group. Error bars represent SEM.

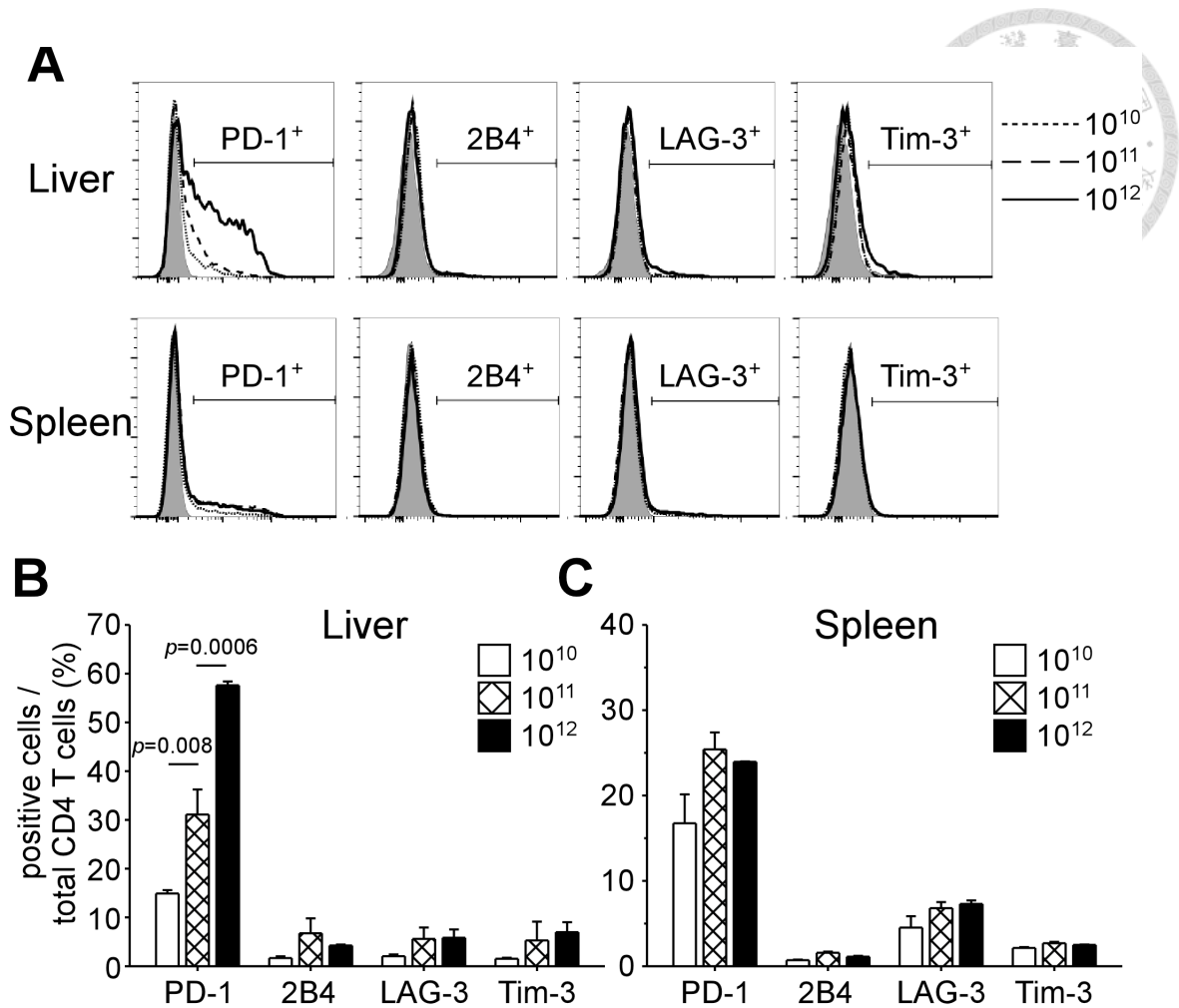


Figure 5. The levels of PD-1 upregulation on intrahepatic CD4 T cells depended on viral loads

Mice were infected with different doses of AAV/HBV and sacrificed 4 months after infection. Lymphocytes in liver and spleen were isolated and analyzed by flow cytometry. The expressions of PD-1, 2B4, LAG-3, and Tim-3 were evaluated after gating on viable TCR β ⁺CD4⁺ cells. (A) Representative data of PD-1, 2B4, LAG-3, and Tim-3 expression on CD4 T cells in the liver and the spleen of mice infected with different loads of AAV/HBV. (B and C) Summary results of PD-1, 2B4, LAG-3, and Tim-3 expression on intrahepatic and splenic CD4 T cells. Data were representative of three independent experiments with 3 to 5 mice per group. Error bars represent SEM.

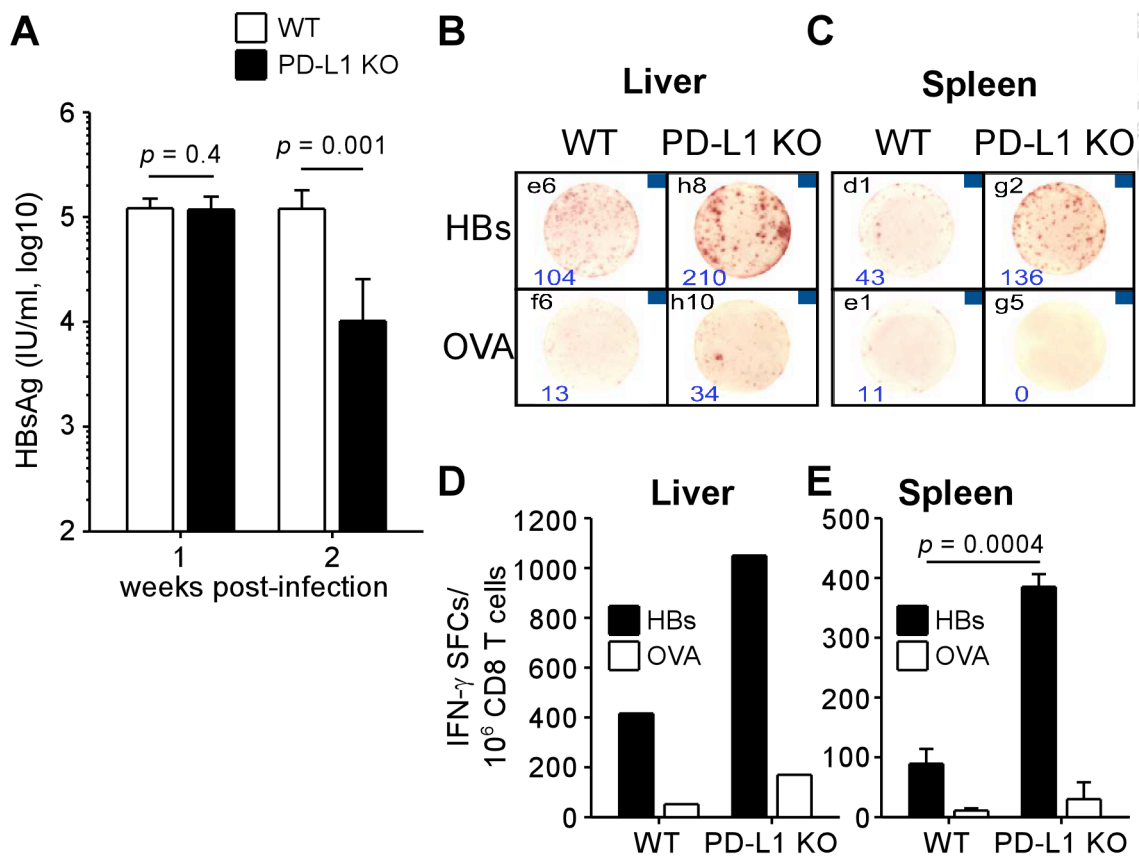


Figure 6. HBV-specific immunity in early stage of infection was more potent in the absence of PD-1:PD-L1

Wild type (WT) and PD-L1 KO mice were infected with 10^{12} vg of AAV/HBV and were sacrificed at week 2 p.i. (A) Sera were collected for the detection of HBsAg by electrochemiluminescence. (B to D) Intrahepatic and splenic CD8 T cells were isolated and subjected to IFN- γ ELISPOT assays. Representative photographs (B and C) and summary results (D and E) are shown. Data are representative of two independent experiments with 4 mice per group. Error bars represent SD.

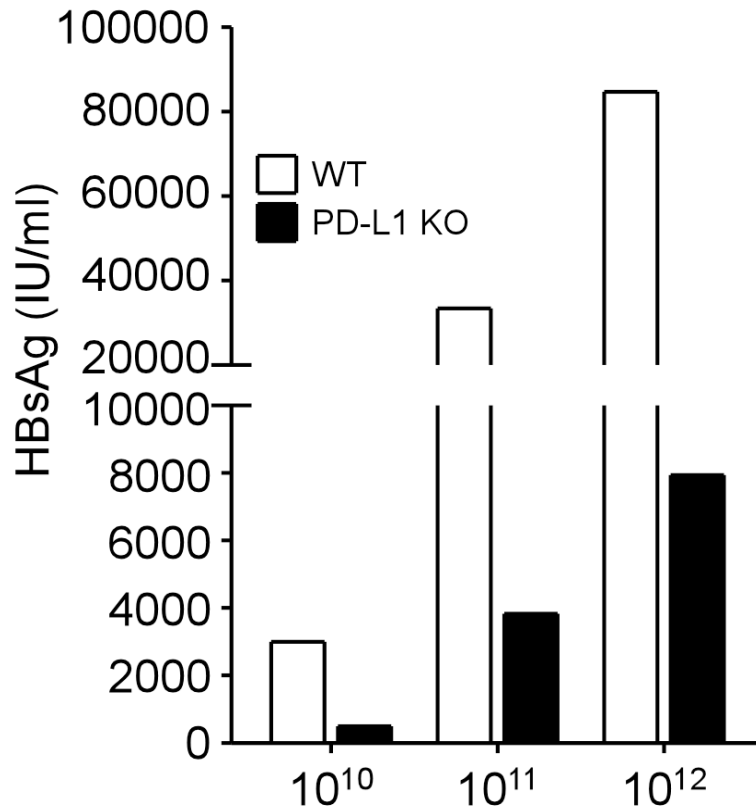


Figure 7. Reduction of HBsAg in PD-L1 KO mice infected with low, intermediate, and high viral loads of AAV/HBV

WT and PD-L1 KO mice were infected with low (10^{10} vg), intermediate (10^{11} vg), or high (10^{12} vg) viral loads of AAV/HBV. Sera were collected at week 2 p.i. to determine the levels of HBsAg by electrochemiluminescence.

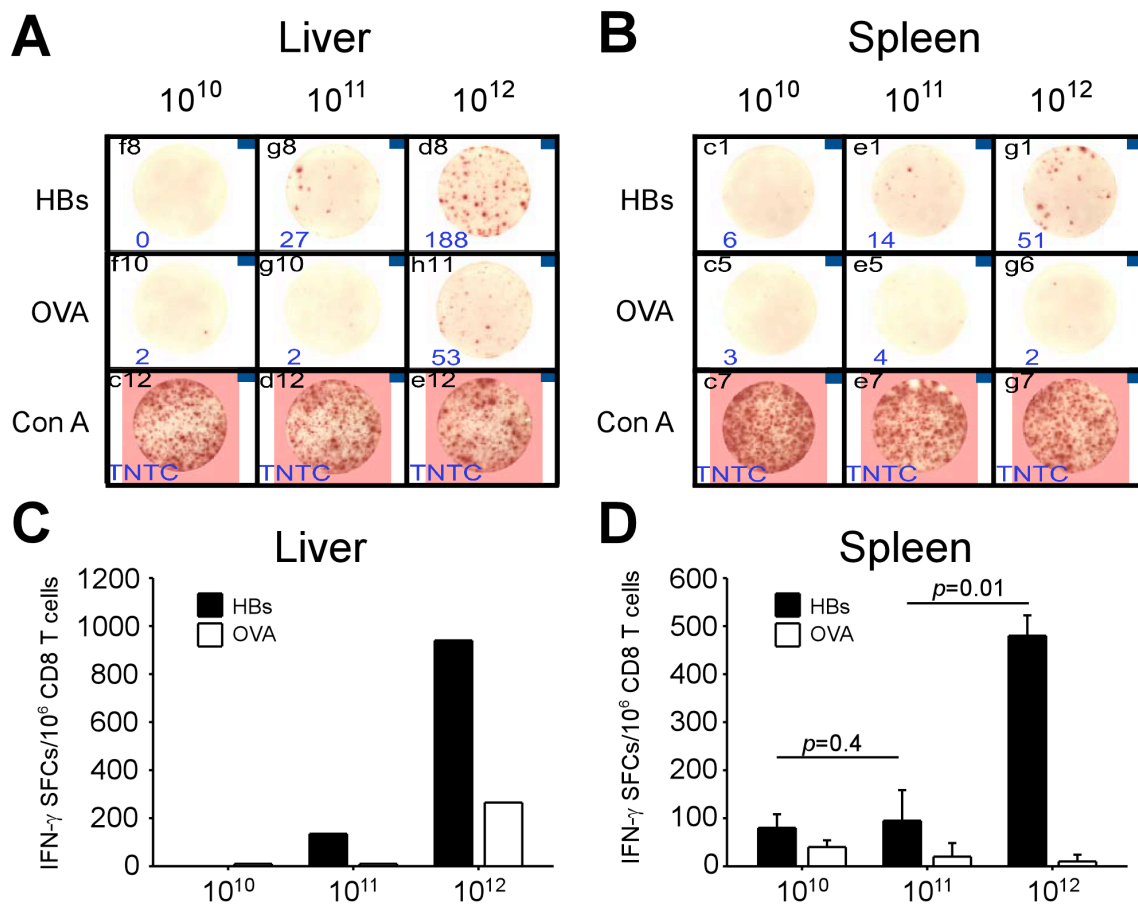


Figure 8. Higher viral loads elicited more intense functions of HBV-specific CD8 T cells in the early phase of infection in PD-L1 KO mice

PD-L1 KO mice were infected with different loads of AAV/HBV (n = 3 mice per group) and sacrificed two weeks p.i. IFN- γ ELISPOT was performed following isolation and enrichment of CD8 T cells from the liver and the spleen. (A and B) Representative data of IFN- γ production by HBV-specific CD8 T cells from the liver and the spleen of KO mice infected with different doses of AAV/HBV. (C and D) Summary results of IFN- γ spot-forming CD8 T cells from the liver and the spleen. Error bars represent SD.

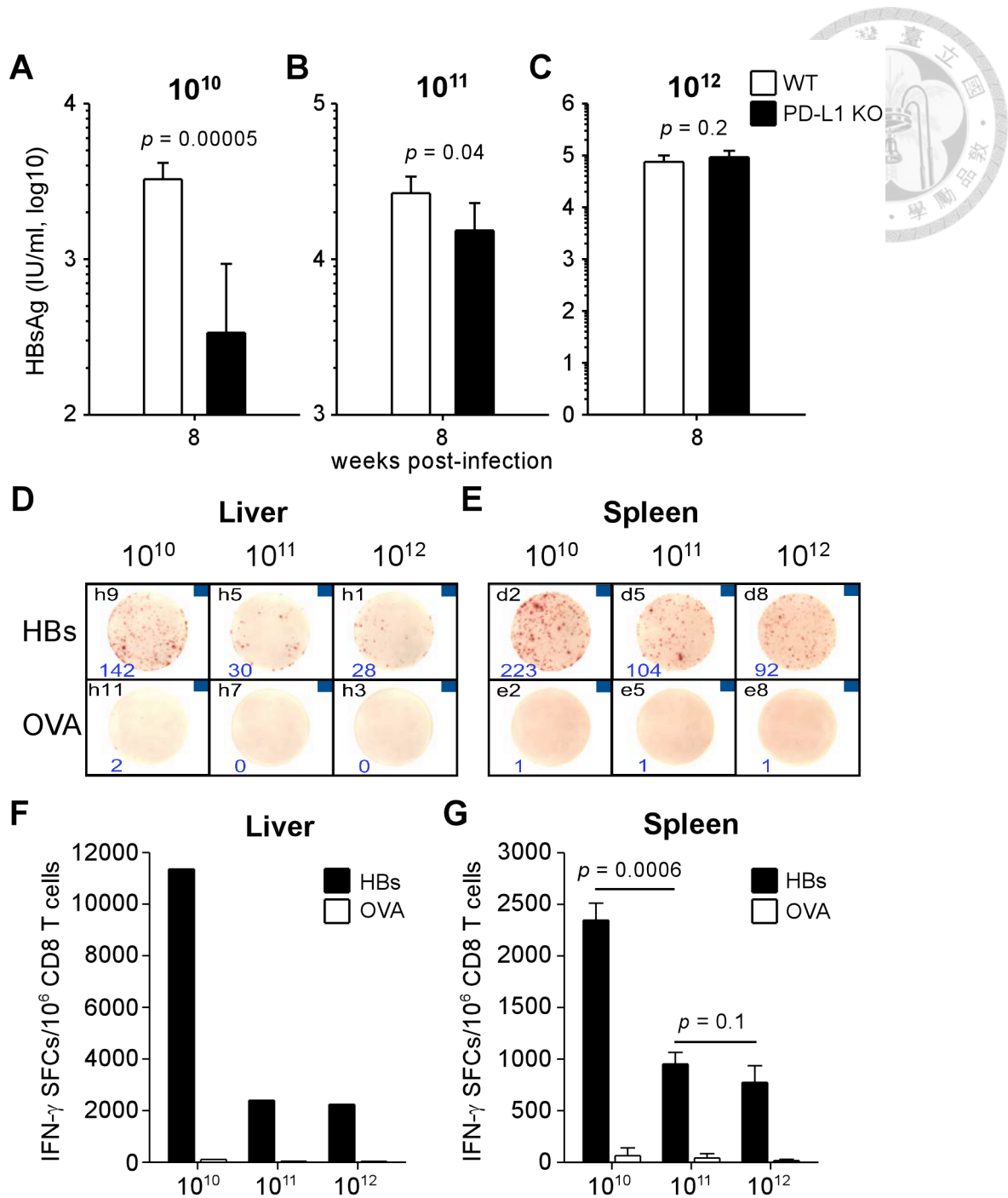
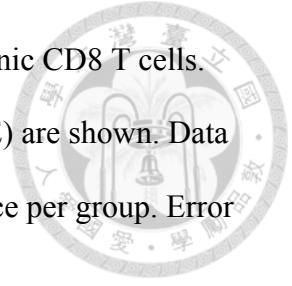


Figure 9. Accelerated functional loss of HBV-specific CD8 T cells in PD-L1 KO mice infected with high viral load of AAV/HBV

Wild type and PD-L1 KO mice were infected with different doses of AAV/HBV. (A to C) Sera were collected at week 8 p.i. for the detection of HBsAg. (D to G) PD-L1 KO mice infected with different doses were immunized and sacrificed as described in

Figure 3. IFN- γ ELISPOT was performed with intrahepatic and splenic CD8 T cells. Representative photographs (B and C) and summary results (D and E) are shown. Data are representative of two independent experiments with at least 3 mice per group. Error bars represent SD.



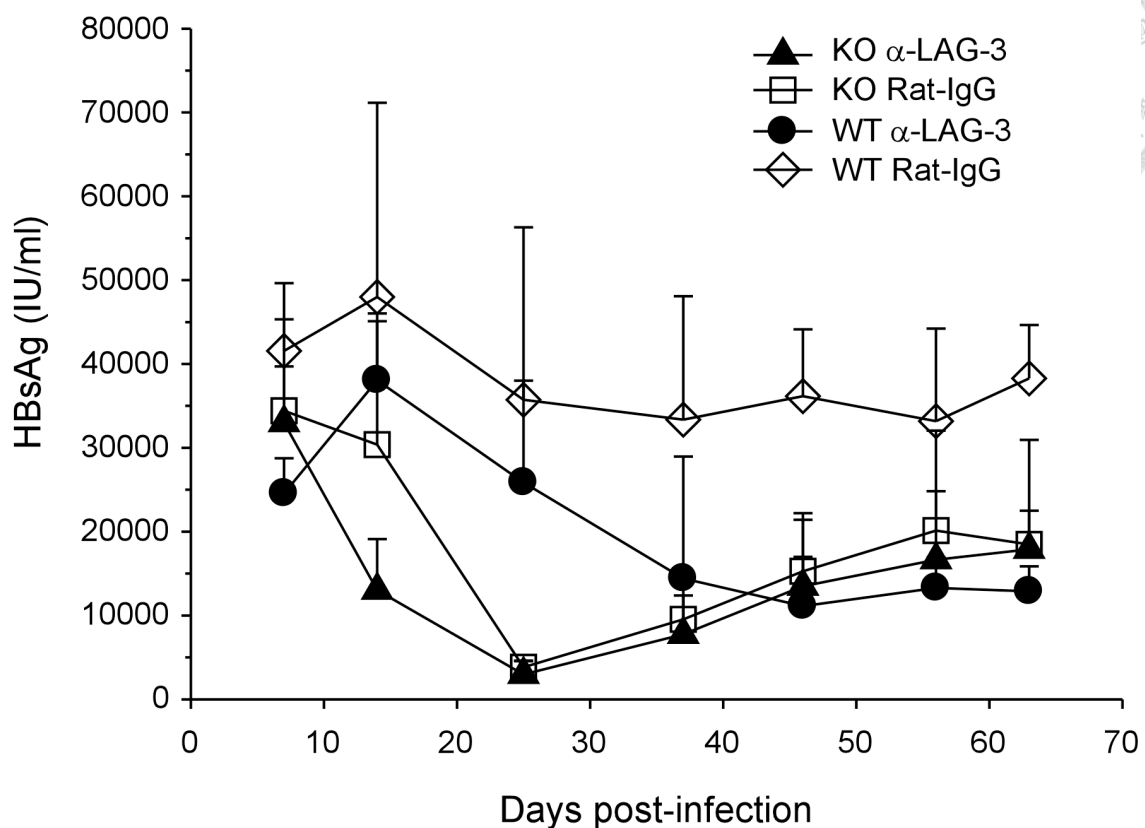


Figure 10. Blockade of LAG-3 accelerated the reduction of serum HBsAg in PD-L1

KO mice

WT and PD-L1 KO mice were i.p. injected with 200 μ g α -LAG-3 monoclonal antibody (mAb) or Rat-IgG isotype control antibody on day -7, -1, 4, 8, 15, 21, 25, 39, 47, 56 (n = 5 mice per group). Seven days after the first antibody injection (day 0), mice were infected with 10^{11} vg of AAV/HBV by i.v. injection. Sera were collected at indicated time for the measurement of HBsAg by electrochemiluminescence. Error bars represent SD.

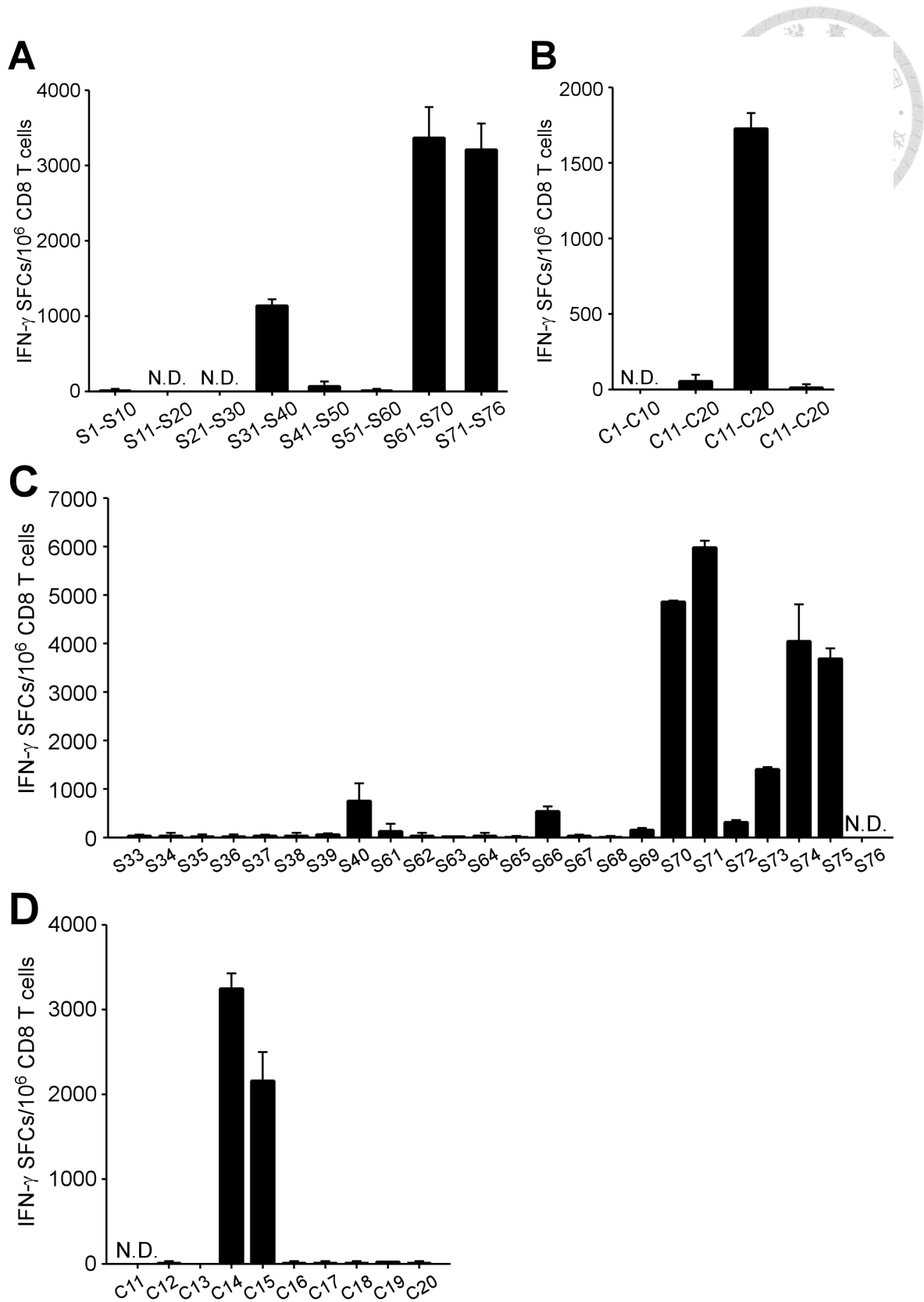


Figure 11. Identification of H-2Kb-restricted dominant epitopes of HBsAg and HBcAg

B6 mice were immunized twice at a two-week interval by intramuscular injection of pHBs and pHBc plasmid DNAs, which encode HBsAg and HBcAg, respectively, followed by electroporation. Splenic CD8 T cells isolated one week after the second immunization were subjected to IFN- γ ELISPOT assays using overlapping peptides shown in Table 1. (A and B) CD8 T cells from immunized mice were co-cultured with EL4 cells that were pulsed with peptide pools. (C and D) Individual peptides from positive pools (S31-S40, S61-S70, S71-S76, and C11-C20) in Figure 11A and B were used to identify the H-2Kb-restricted epitopes. N.D., not detected.

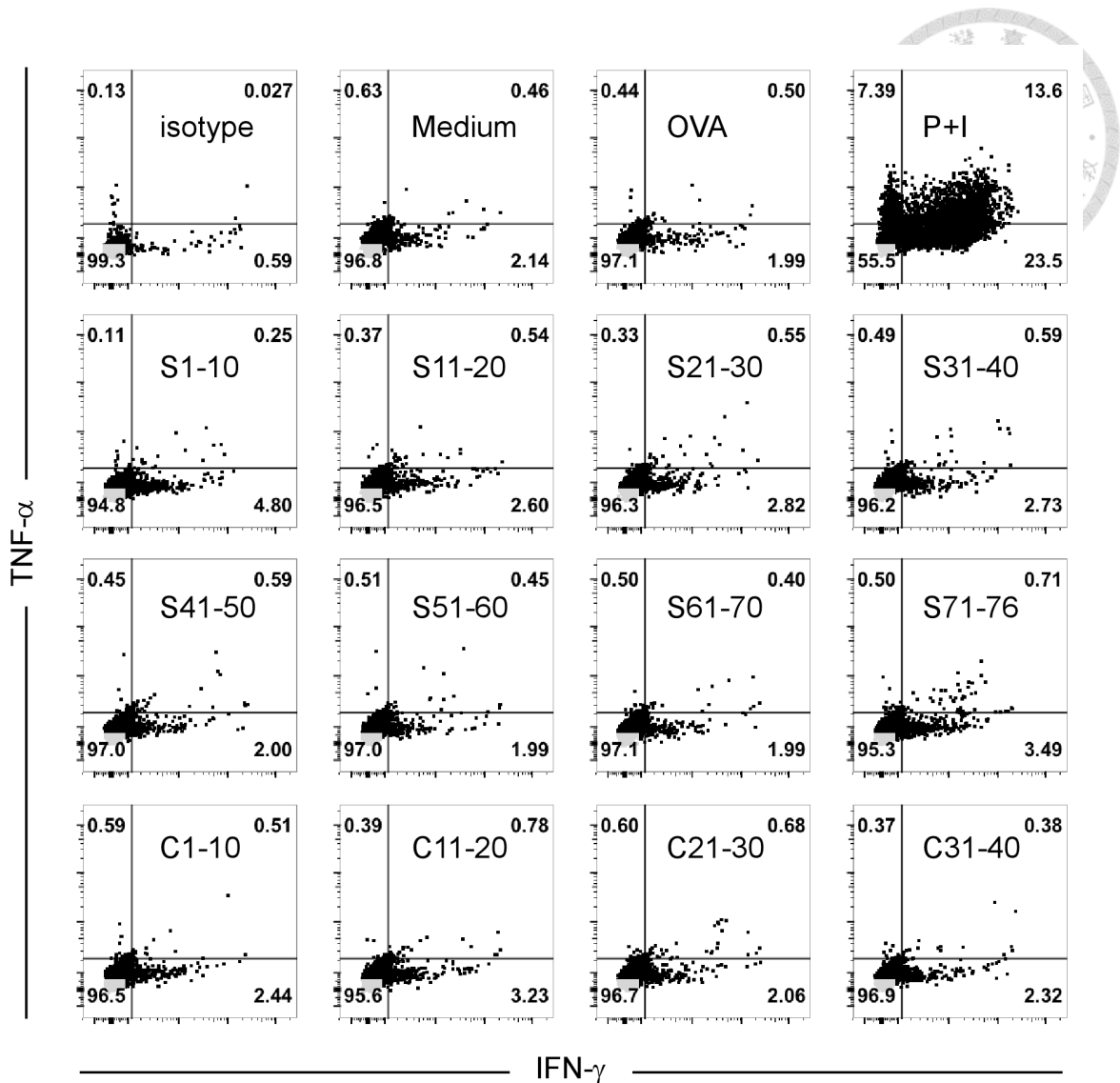


Figure 12. Detection of subdominant clones of HBV-specific CD8 T cells in chronically infected C57BL/6 mice

Intrahepatic CD8 T cells, which were pooled from 5 B6 mice infected with 10^{11} vg AAV/HBV for 12 months, were co-cultured with EL4 cells pulsed with overlapping peptide pools. After 6 hours of culture in the presence of BFA, the productions of IFN- γ and TNF- α by total intrahepatic CD8 T cells (gated on viable TCR β^+ CD8 $^+$ cells) were detected by flow cytometry following intracellular cytokine staining. Stimulations with EL4 cells pulsed with OVA peptide or RPMI medium alone served as negative control, while PMA plus ionomycin (P+I) stand for positive stimulation.

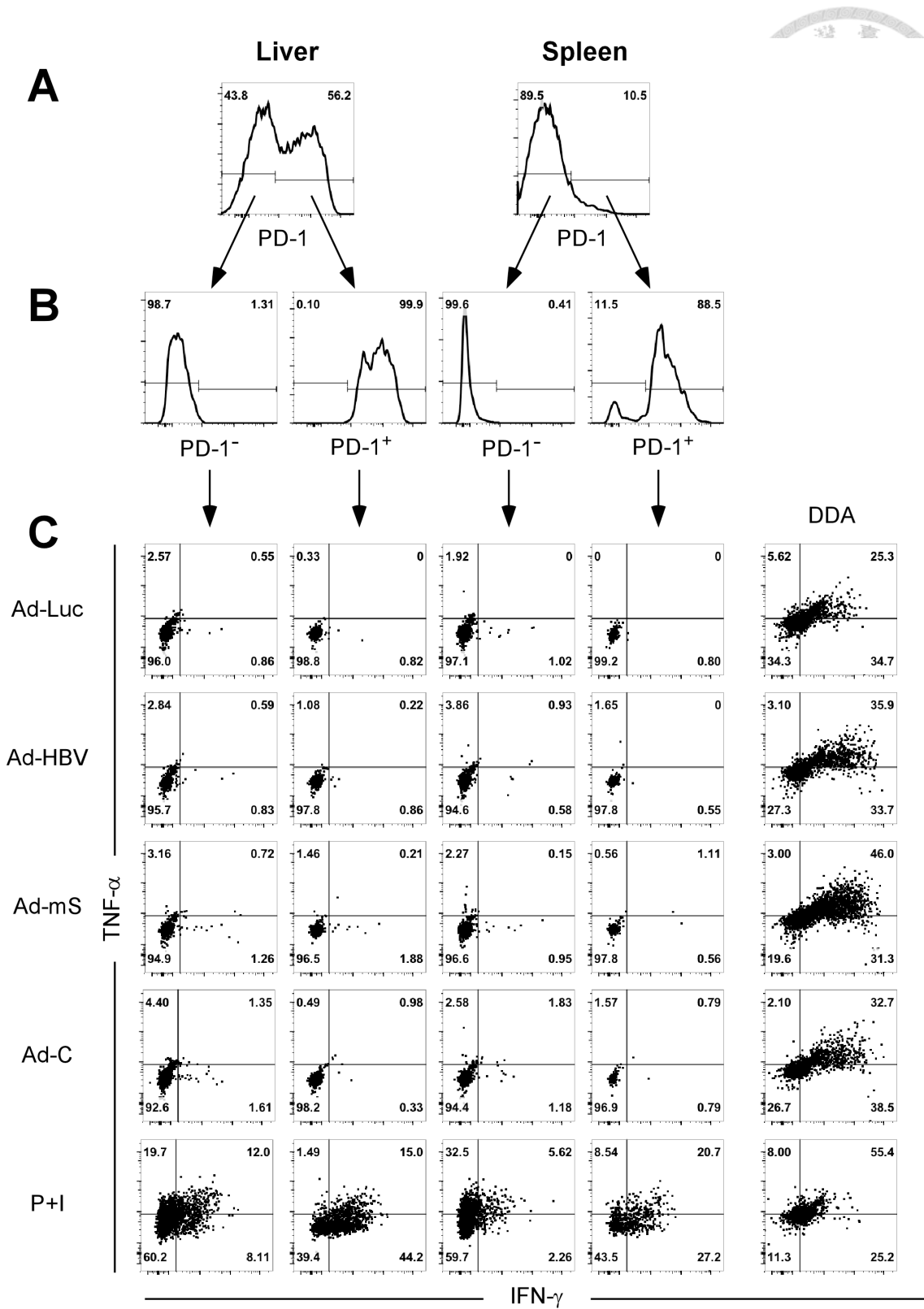


Figure 13. PD-1⁺ CD8 T cells from AAV/HBV-infected mice were irresponsive to stimulation using bone marrow-derived dendritic cells (BMDCs) infected with

adenoviral vectors expressing HBV antigens

Mice (n = 7) were infected with 10^{12} vg AAV/HBV and sacrificed 6 weeks later. Pooled intrahepatic and splenic CD8 T cells were enriched by MACS beads and sorted by FACSaria following PD-1 staining. (A) PD-1 expression on CD8 T cells in the liver and the spleen of AAV/HBV infected mice. (B) PD-1 expression on CD8 T cells after sorting. (C) Bone marrow-derived dendritic cells (BMDCs) from PD-L1 KO mice were infected with 50 MOI of adenoviral vectors expressing luciferase (Ad-Luc), HBV (Ad-HBV), pre-S1 envelope protein (Ad-mS), or core protein (Ad-C). After 24 hours, infected BMDCs were washed and co-cultured with sorted CD8 T cells for HBV-specific stimulation. Ad-Luc group served as a background control of responses against adenoviral vectors. Splenic CD8 T cells from mice immunized by twice DNA immunization and one adenoviral boost (DDA) were used as positive control for HBs- and HBc-specific responses. The production of IFN- γ and TNF- α by sorted CD8 T cells were detected by flow cytometry after intracellular cytokine staining.

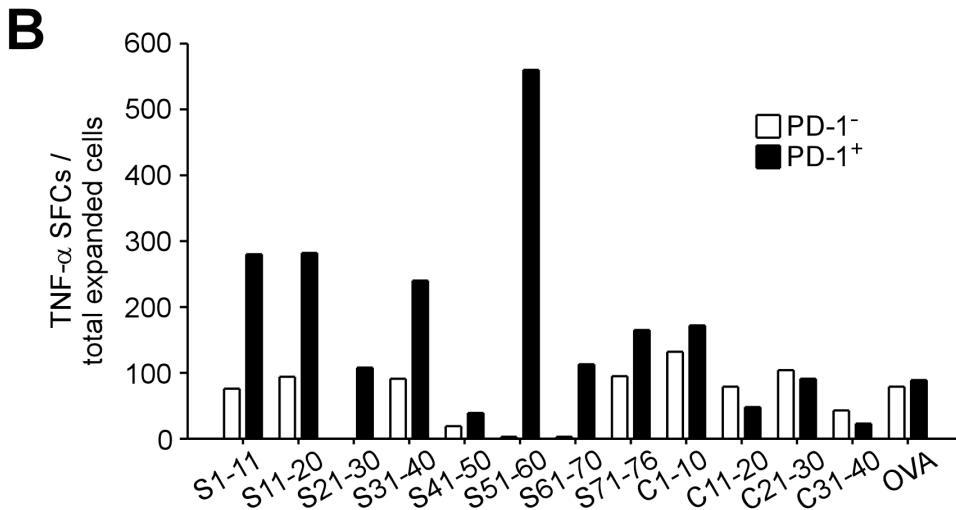
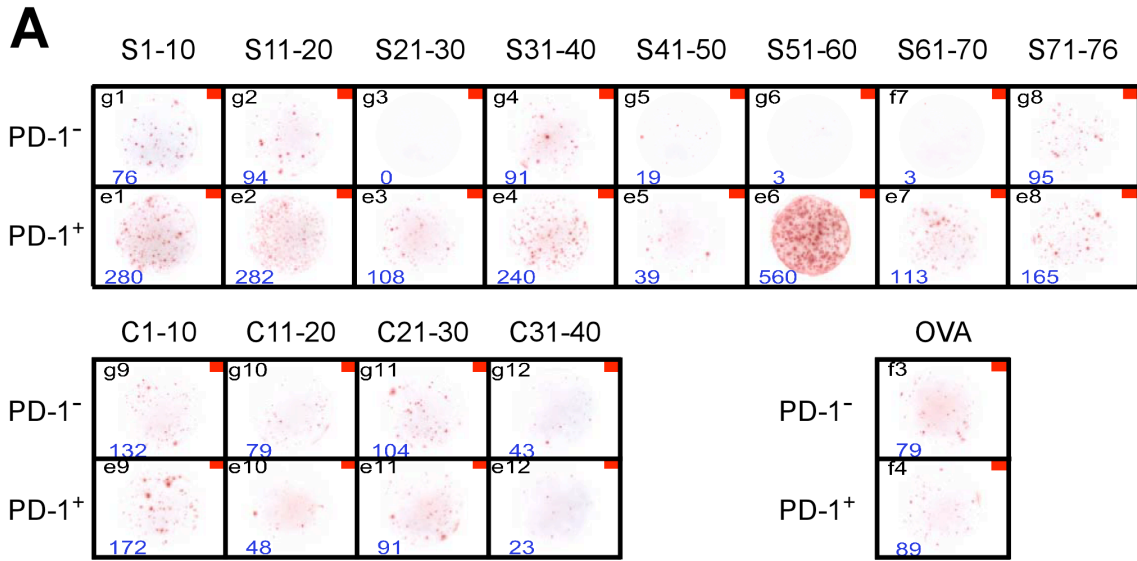


Figure 14. PD-1⁺ intrahepatic CD8 T cells showed more intense function of TNF- α production against HBV peptides than the PD-1⁻ counterpart CD8 T cells after *in vitro* expansion

Mice were infected with 10^{12} vg AAV/HBV and sacrificed 6 weeks later. Intrahepatic CD8 T cells were enriched by MACS beads and sorted by FACSARIA following PD-1 staining. Sorted CD8 T cells were co-cultured with BMDCs and irradiated naïve splenocytes pulsed with overlapping peptide pools. On day 10, cells were restimulated with peptide-pulsed irradiated naïve splenocytes. Cells were subjected to TNF- α

ELISPOT assay on day 20 with the stimulation of peptide-pulsed EL4 cells for 24 hours. OVA peptide served as a negative stimulation. (A) Representative data of TNF- α production by PD-1⁺ and PD-1⁻ intrahepatic CD8 T cells after *in vitro* expansion. (B) Summary results of TNF- α production by *in vitro* expanded PD-1⁺ and PD-1⁻ intrahepatic CD8 T cells of AAV/HBV-infected mice.

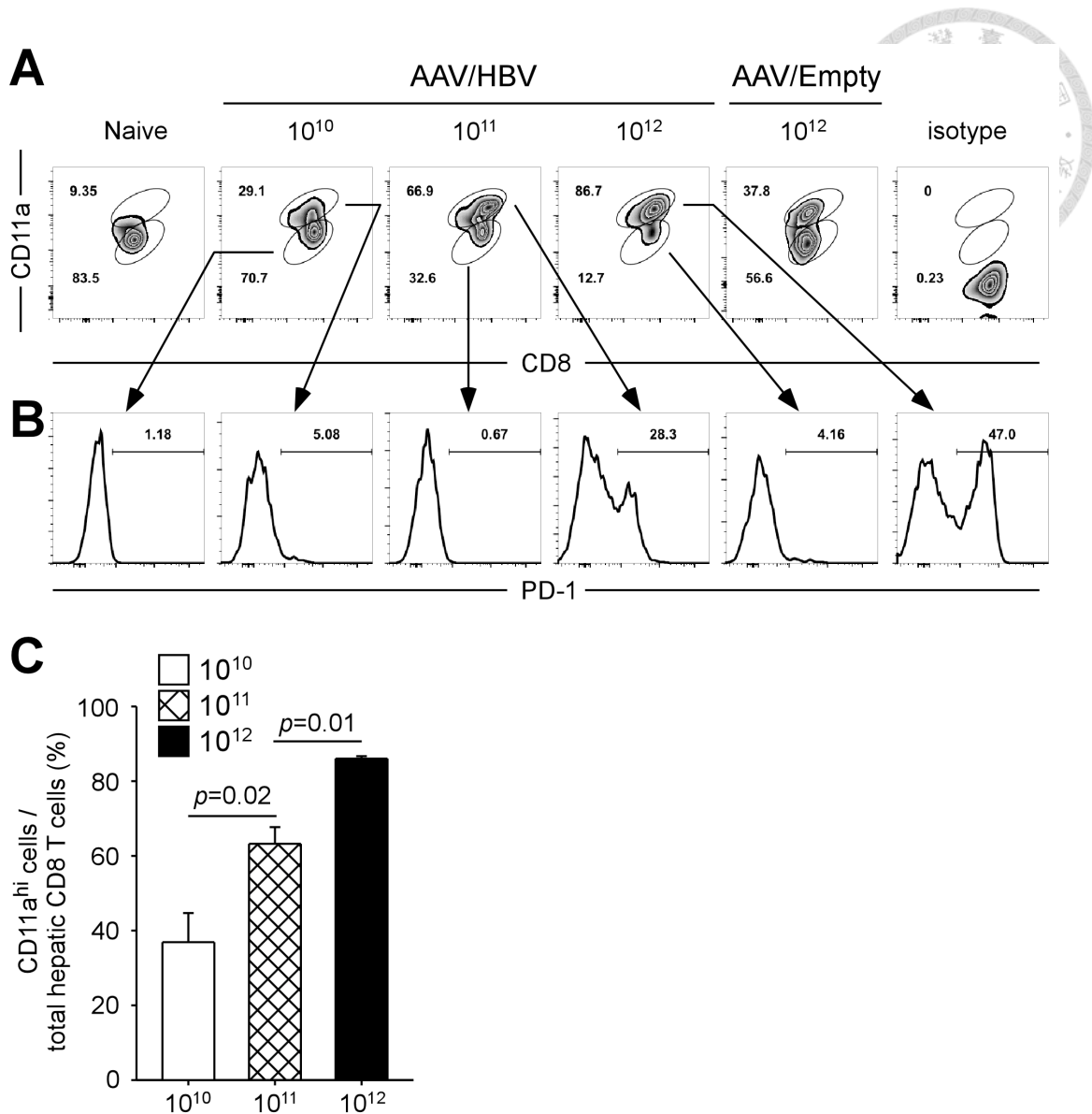
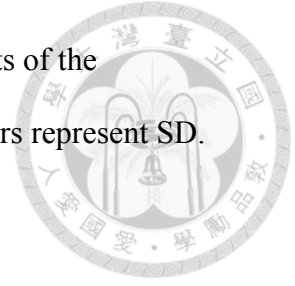


Figure 15. The frequencies of CD11a^{hi} CD8 T cells depended on viral loads of AAV/HBV

Mice were infected with different doses of AAV/HBV and sacrificed 4 months after infection. Intrahepatic lymphocytes were isolated and analyzed for surrogate activation markers by flow cytometry. TCR β ⁺CD8⁺ cells were gated for the analysis of CD11a^{hi} CD8 T cells. AAV/Empty served as a negative control. (A) Representative data of the frequencies of CD11a^{hi} cells among CD8 T cells in the liver of mice infected with different doses of AAV/HBV and age-matched naïve mice. (B) PD-1 expression on

CD11a^{hi} and CD11a^{low} intrahepatic CD8 T cells. (C) Summary results of the percentages of CD11a^{hi} cells in total intrahepatic CD8 cells. Error bars represent SD.



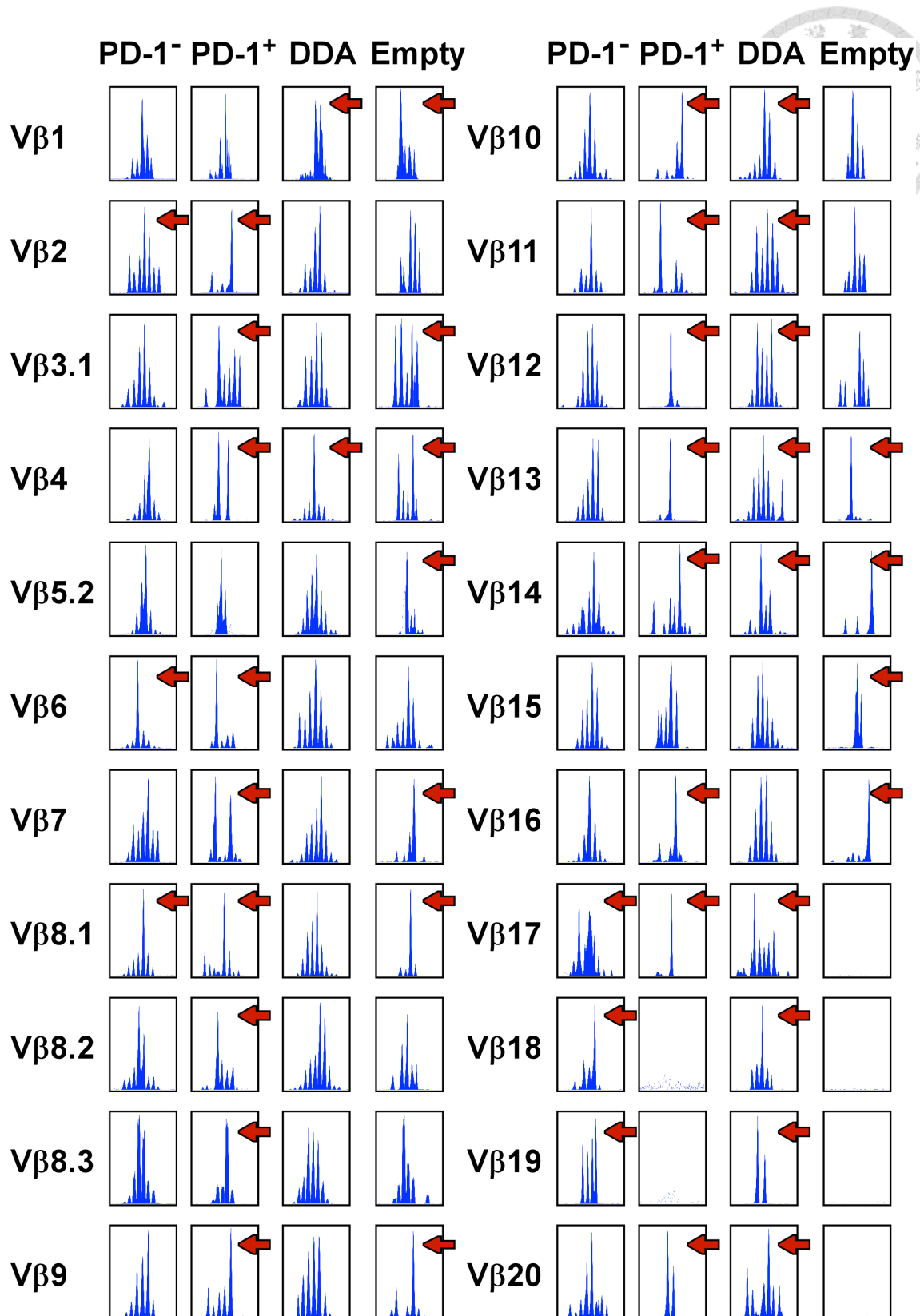
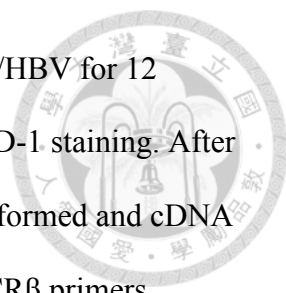


Figure 16. Higher degree of oligoclonal T-cell expansion was observed in PD-1⁺ intrahepatic CD8 T cells than that of the PD-1⁻ counterpart CD8 T cells



Intrahepatic CD8 T cells from 5 B6 mice infected with 10^{11} vg AAV/HBV for 12 months were pooled, enriched, and sorted by FACS Aria following PD-1 staining. After RNA extraction from sorted cells, reverse transcription PCR was performed and cDNA products were subjected to PCR reactions using different forward TCR β primers (V β 1-20) with one reverse C β primer described in Table 2. The PCR products of TCR β sequences were labeled with FAM fluorochrome by primer extension using C β -FAM primer shown in Table 2. The lengths of TCR β cDNA fragments were analyzed by ABI3700 Analyzer and PeakScanner Software. Arrows indicate peaks differed from Gaussian distribution profile and represent the presences of oligoclonal T-cell expansions. Panels showed no signals resulted from inadequate amounts of PCR products. Mice immunized with plasmid DNA and adenoviral vector (DDA) served as positive control, and those infected with AAV/Empty (Empty) served as negative control.



Table 1. Overlapping peptide library of HBsAg and HBcAg

Peptide	pre-S1/pre-S2/Surface (389 aa)	
	Location	Amino acid sequence
S1	HBs 1-15	MGQNLSTSNPLGFFP
S2	HBs 6-20	STSNPLGFFPDHQLD
S3	HBs 11-25	LGFFPDHQLDPAFRA
S4	HBs 16-30	DHQLDPAFRANTANP
S5	HBs 21-35	PAFRANTANPDWDFN
S6	HBs 26-40	NTANPDWDFNPNKDT
S7	HBs 31-45	DWDFNPNKDTWPDAN
S8	HBs 36-50	PNKDTWPDANKVGAG
S9	HBs 41-55	WPDANKVGAGAFGLG
S10	HBs 46-60	KVGAGAFGLGFTPPH
S11	HBs 51-65	AFGLGFTPPHGLLG
S12	HBs 56-70	FTPPHGLLGWSPQA
S13	HBs 61-75	GLLGWSPQAQGILQ
S14	HBs 66-80	WSPQAQGILQTLPAN
S15	HBs 71-85	QGILQTLPANPPPAS
S16	HBs 76-90	TLPANPPPASTNRQS
S17	HBs 81-95	PPPASTNRQSGRQPT
S18	HBs 86-100	TNRQSGRQPTPLSPP
S19	HBs 91-105	GRQPTPLSPPLRNTH
S20	HBs 96-110	PLSPPLRNTHPQAMQ
S21	HBs 101-115	LRNTHPQAMQWNSTT
S22	HBs 106-120	PQAMQWNSTTFHQTL
S23	HBs 111-125	WNSTTFHQTLDQPRV
S24	HBs 116-130	FHQTLDQPRVRGLYF
S25	HBs 121-135	QDPRVRGLYFPAGGS
S26	HBs 126-140	RGLYFPAGGSSSGTV
S27	HBs 131-145	PAGGSSSGTVNPVLT
S28	HBs 136-150	SSGTVNPVLT TASPL
S29	HBs 141-155	NPVLT TASPLSSIFS
S30	HBs 146-160	TASPLSSIFSRIGDP
S31	HBs 151-165	SSIFSRIGDPALNME
S32	HBs 156-170	RIGDPALNMENITSG
S33	HBs 161-175	ALNMENITSGFLGPL
S34	HBs 166-180	NITSGFLGPLLVLQA
S35	HBs 171-185	FLGPLLVLQAGFFLL
S36	HBs 176-190	LVLQAGFFLLTRILT
S37	HBs 181-195	GFFLLTRILTIPQSL

S38	HBs 186-200	TRILTIPQSLDSWWT
S39	HBs 191-205	IPQSLDSWWTSLNFL
S40	HBs 196-210	DSWWTSLNFLGGTTV
S41	HBs 201-215	SLNFLGGTTVCLGQN
S42	HBs 206-220	GGTTVCLGQNSQSPT
S43	HBs 211-225	CLGQNSQSPTSNHSP
S44	HBs 216-230	SQSPTSNHSP TSCPP
S45	HBs 221-235	SNHSP TSCPPTCPGY
S46	HBs 226-240	TSCPPTCPGYRWMCL
S47	HBs 231-245	TCPGYRWMCLRRFII
S48	HBs 236-250	RWMCLRRFIIIFLFIL
S49	HBs 241-255	RRFIIIFLIFLLCLI
S50	HBs 246-260	FLFIFLLCLIFLLVL
S51	HBs 251-265	LLCLIFLLVLLDYQG
S52	HBs 256-270	FLLVLLDYQGMPLVC
S53	HBs 261-275	LDYQGMPLVCPPIPG
S54	HBs 266-280	MPLVCPPIPGSSTTS
S55	HBs 271-285	PLIPGSSTTSTGPCR
S56	HBs 276-290	SSTTSTGPCRTCMTT
S57	HBs 281-295	TGPCRTCMTTAQGTS
S58	HBs 286-300	TCMTTAQGTSMYPSC
S59	HBs 291-305	AQGTSMYPSCCCTKP
S60	HBs 296-310	MYPSCCCTKPSDGNC
S61	HBs 301-315	CCTKPSDGNCTCIPI
S62	HBs 306-320	SDGNCTCIPIPSSWA
S63	HBs 311-325	TCIPIPSSWAFGKFL
S64	HBs 316-330	PSSWAFGKFLWEWAS
S65	HBs 321-335	FGKFLWEWASARFSW
S66	HBs 326-340	WEWASARFSWLSLLV
S67	HBs 331-345	ARFSWLSLLVFPVQW
S68	HBs 336-350	LSLLVFPVQWFVGLS
S69	HBs 341-355	PFVQWFVGLSPTVWL
S70	HBs 346-360	FVGLSPTVWLSVIWM*
S71	HBs 351-365	PTVWLSVIWMMWYWG*
S72	HBs 356-370	SVIWMMWYWGPSLYS
S73	HBs 361-375	MWYWGPSLYSILSPF
S74	HBs 366-380	PSLYSILSPFLPLLP*
S75	HBs 371-385	ILSPFLPLLP ^I FFCL*
S76	HBs 376-389	LPLLP ^I FFCLWVYI





Precore/Core (212 aa)		
Peptide	Location	Amino acid sequence
C1	HBc 1-15	MQLFHLCLIISCSCP
C2	HBc 6-20	LCLIISCSCPTVQAS
C3	HBc 11-25	SCSCPTVQASKLCLG
C4	HBc 16-30	TVQASKLCLGWLWGM
C5	HBc 21-35	KLCLGWLWGM DIDPY
C6	HBc 26-40	WLWGM DIDPYKEFGA
C7	HBc 31-45	DIDPYKEFGATVELL
C8	HBc 36-50	KEFGATVELLSFLPS
C9	HBc 41-55	TVELLSFLPSDFFPS
C10	HBc 46-60	SFLPSDFFPSVRDLL
C11	HBc 51-65	DDFFPSVRDLLDTASA
C12	HBc 56-70	VRDLLDTASALYREA
C13	HBc 61-75	DTASALYREALESPE
C14	HBc 66-80	LYREALESPEHCSPH
C15	HBc 71-85	LESPEHCSPHHTALR
C16	HBc 76-90	HCSPHHTALRQAILC
C17	HBc 81-95	HTALRQAILCWGELM
C18	HBc 86-100	QAILCWGELMTLATW
C19	HBc 91-105	WGELMTLATWVGVNL
C20	HBc 96-110	TLATWVGVNLEDPAS
C21	HBc 101-115	VGVNLEDPASRDVV
C22	HBc 106-120	EDPASRDVVSYVNT
C23	HBc 111-125	RDLVVS YVNTNMGLK
C24	HBc 116-130	SYVNTNMGLKFRQLL*
C25	HBc 121-135	NMGLKFRQLLWFHIS*
C26	HBc 126-140	FRQLLWFHISCLTFG
C27	HBc 131-145	WFHISCLTFGRETVI
C28	HBc 136-150	CLTFGRETVIEYLV
C29	HBc 141-155	RETVIEYLV SFGVWI
C30	HBc 146-160	EYLV SFGVWIRTPPA
C31	HBc 151-165	FGVWIRTPPAYRPPN
C32	HBc 156-170	RTPPAYRPPNAPILS
C33	HBc 161-175	YRPPNAPILSTLPET
C34	HBc 166-180	APILSTLPETT VVRR
C35	HBc 171-185	TLPETTVVRRRGRSP
C36	HBc 176-190	TVVRRRGRSPRRRTP
C37	HBc 181-195	RGRSPRRRTPSPRRR
C38	HBc 186-200	RRRTPSPRRRRSQSP
C39	HBc 191-205	SPRRRRSQSPRRRRS
C40	HBc 196-212	RSQSPRRRRSQSRESQC

*Underlined sequences are epitopes reported in previous studies.



Table 2. Primers for TCR β spectratype analysis

Primer	Sequences
V β 1	CTGAATGCCCGAGACAGCTCCAAGC
V β 2	TCACTGATACGGAGCTGAGGC
V β 3.1	CCTTGCAGCCTAGAAATTCAGT
V β 4	GCCTCAAGTCGCTTCCAACCTC
V β 5.2	AAGGTGGAGAGAGACAAAGGATTC
V β 6	CTCTCACTGTGACATCTGCCC
V β 7	TACAGGGTCTCACGGAAGAAGC
V β 8.1	GGCTGATCCATTACTCATATGTC
V β 8.2	TCATATGGTGCTGGCAGCACTG
V β 8.3	TGCTGGCAACCTTCGAATAGGA
V β 9	TCTCTCTACATTGGCTCTGCAGGC
V β 10	ATCAAGTCTGTAGAGCCGGAGGA
V β 11	GCACTCAACTCTGAAGATCCAGAGC
V β 12	GATGGTGGGGCTTTCAAGGATC
V β 13	AGGCCTAAAGGAACTAACTCCACT
V β 14	ACGACCAATTCATCCTAAGCAC
V β 15	CCCATCAGTCATCCCAACTTATCC
V β 16	CACTCTGAAAATCCAACCCAC
V β 17	CTAAGTGTTCCTCGAACTCAC
V β 18	CAGCCGGCCAAACCTAACATTCTC
V β 19	CTGCTAAGAAACCATGTACCA
V β 20	TCTGCAGCCTGGGAATCAGAA
C β	AAGCACACGAGGGTAGCCT
C β -FAM	FAM-TTGGGTGGAGTCACATTTCTC